Exploring New Physics with SMEFT and the Impact of Electroweak Perturbative Corrections

Shankha (IMSc, Chennai)

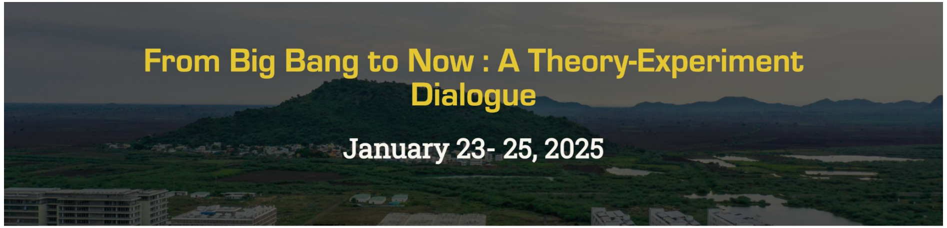

THE INSTITUTE OF MATHEMATICAL SCIENCES

SRM UNIVERSITY AP
Andhra Pradesh

The Standard Model of Particle Physics

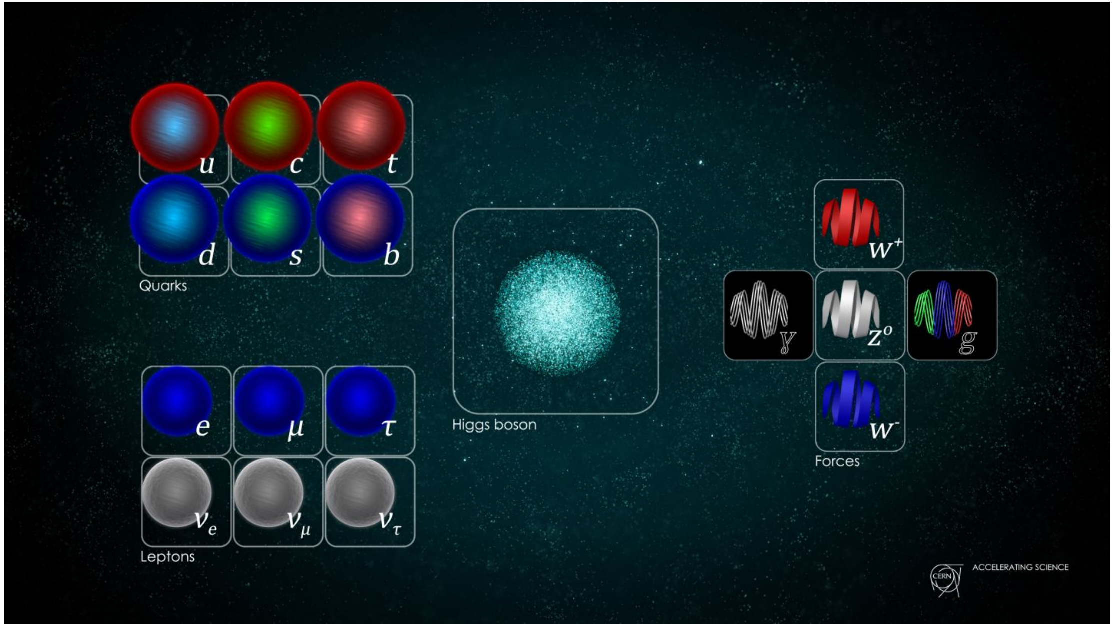

Elementary particles in the Standard Model of particle physics
Image: Daniel Dominguez/CERN

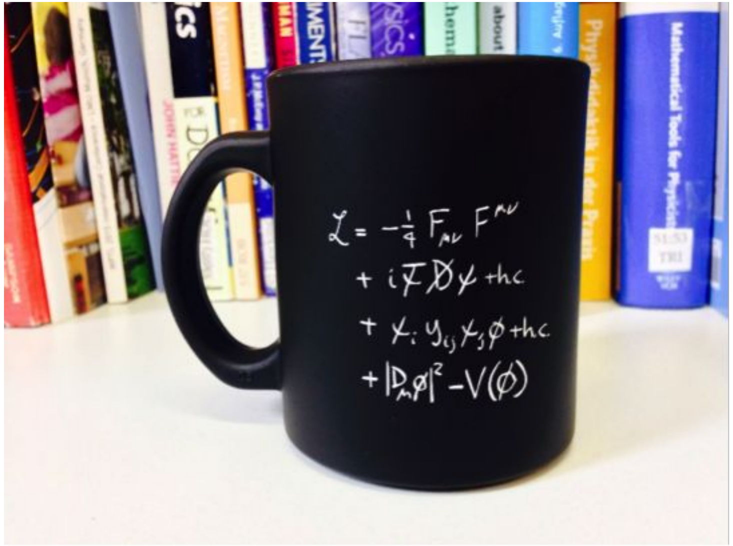

Simplified way of expressing interactions between the Standard Model particles
CERN coffee mug

Importance of precision: the premise

For an insightful discussion on BSM physics, check Biplob da's slides!

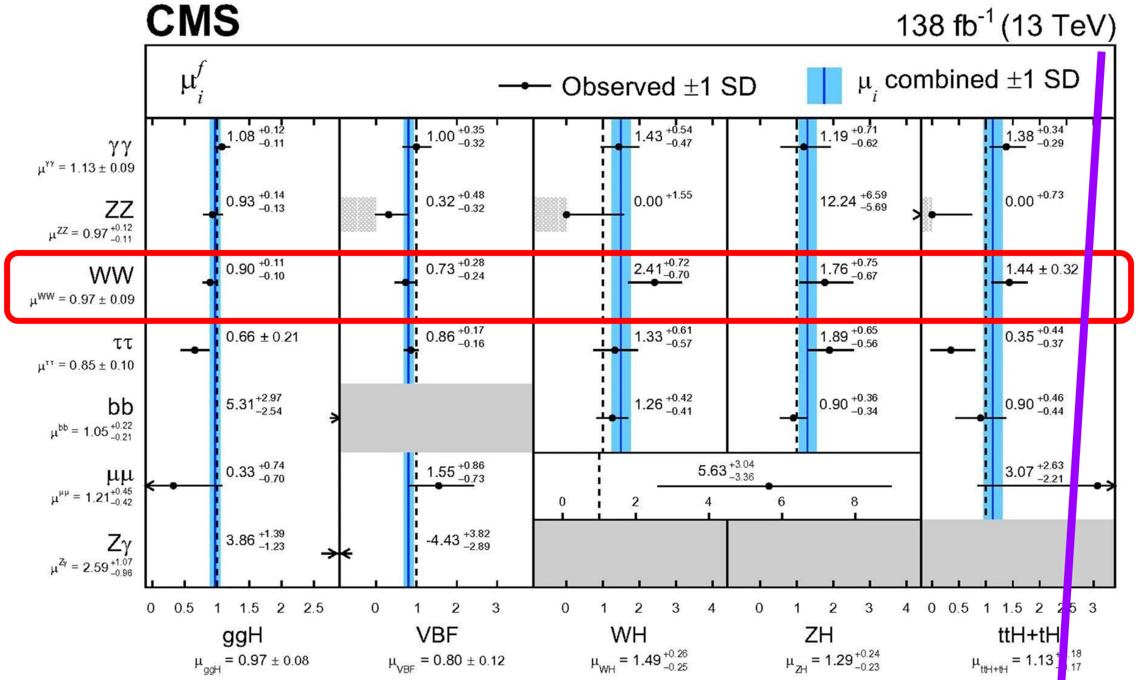

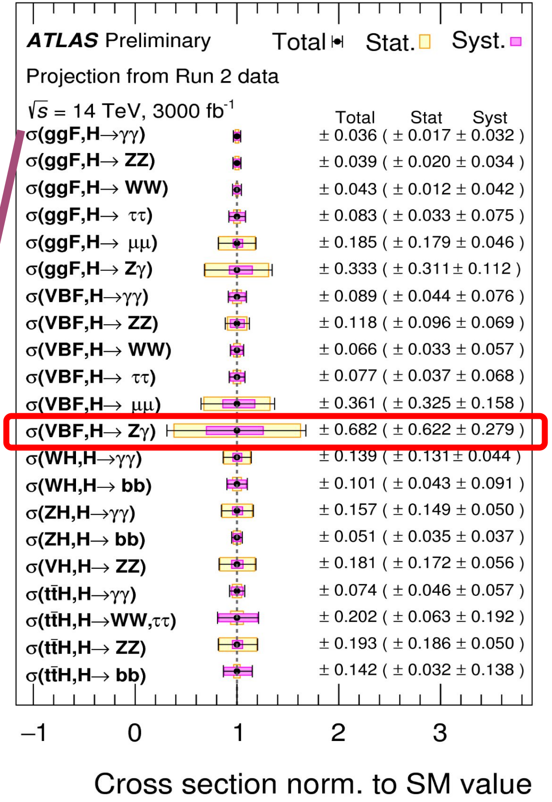

Ratios of the Higgs boson's measured interactions to other particles to its Standard Model expectations. If Standard Model predictions are exact, these numbers would eventually be 1.

From current data

Future projections from LHC, CERN

Importance of precision: the premise

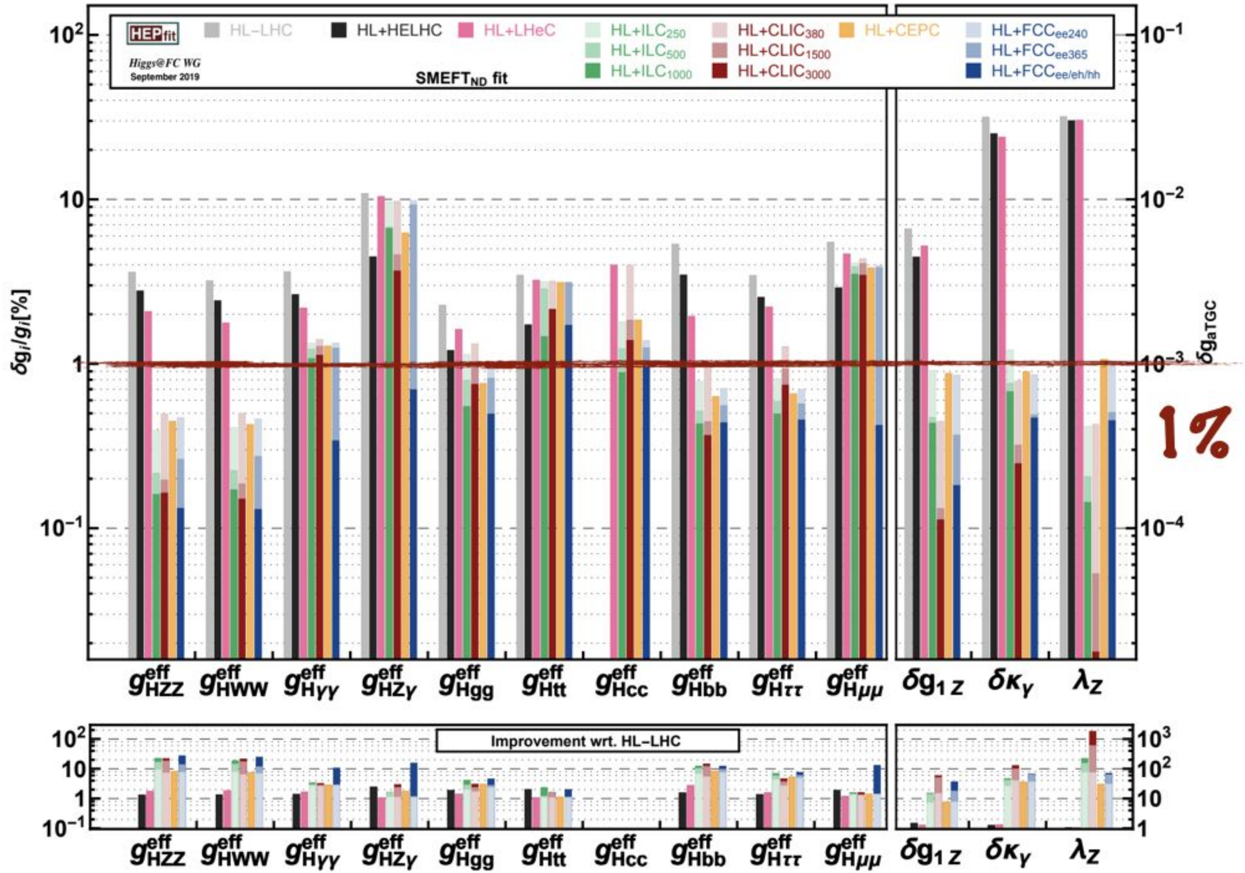

Types of uncertainties in particle physics

- **Systematic (experimental):** instrumental uncertainties, uncertainties due to calibration of energy scales and resolution of detectors, uncertainties on detector efficiencies, etc.
- **Statistical (experimental):** stems from finite number of events recorded
- **Modelling of signal and backgrounds (theoretical):** PDF, scale, more …
- **Luminosity:** uncertainty on precise determination of the rate of collisions
- **Monte Carlo Simulation**

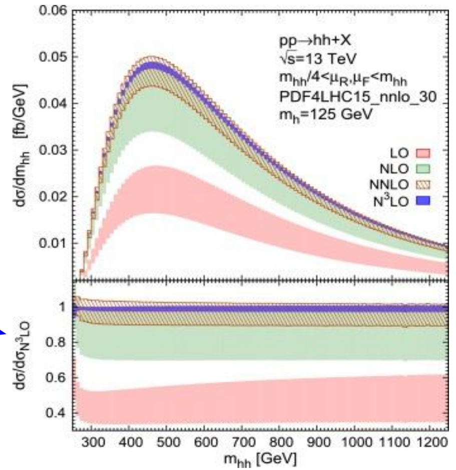

Theory precision ⟺ Experimental precision

Particle physics discovery: the types

Discovery through resonance (the tested paradigm)

We are in the phase of no resonance discoveries since the last 12+ years after the Higgs in 2012. What to do then?

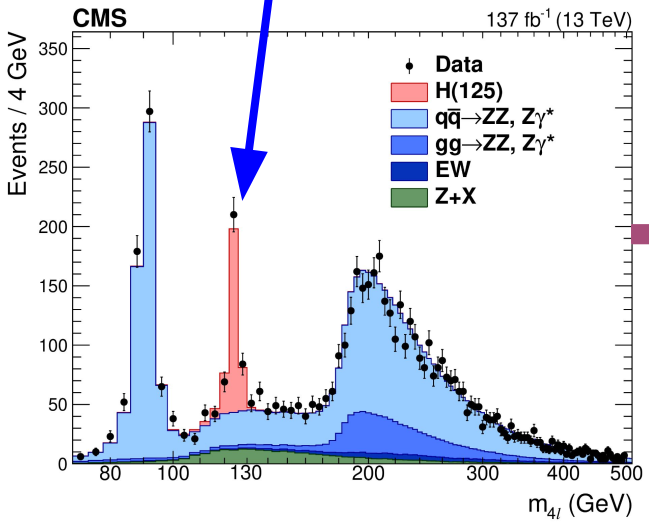

New paradigm!

Discovery through precision

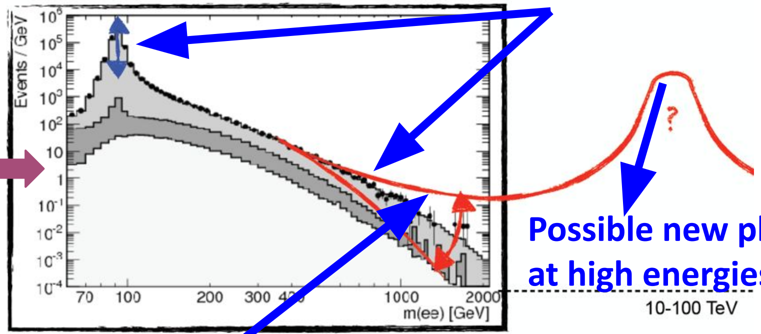

Possible new physics at high energies

Image: Francesco Riva

%-level precision

Possible to see hints of new physics through difference in heights, angular structure and tails of distributions without seeing the actual resonance

Model theistic versus Model agnostic (EFT) approaches

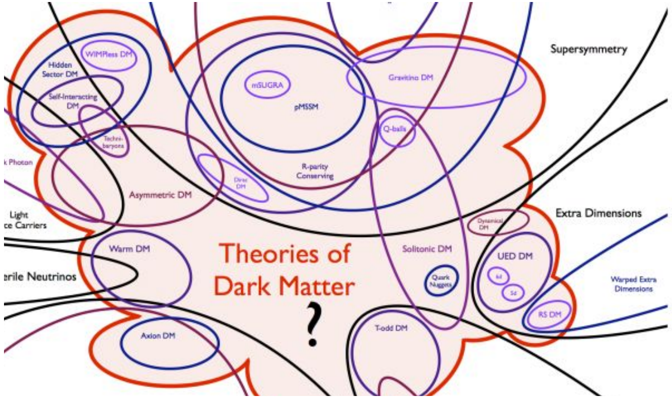

Image: Tim Tait

No direct hints towards new physics explaining the various observations which require physics beyond the Standard Model.

No consensus. Every model comes with additional baggage which needs to be discovered.

Is new physics **hiding somewhere** that we are obviously missing?

Is the **reach just above the present experimental reach**?

Are the **interactions with Standard Model particles extremely feeble**?

Are the **theoretical and experimental precisions not good enough**?

Imprints of new physics could show up as tiny deviations in standard measurements → Hint towards new physics?

Theory precision is thus crucial to minimise uncertainties.

The EFT picture

... is reinforced by the current experimental situation

Image: Admir Greljo

$$\boxed{\mathcal{L} = \mathcal{L}_{SM}^{d=4} + \sum_{d\geq 5} \sum_{i} \frac{c_i}{\Lambda^{d-4}} \mathcal{O}_i^d}$$

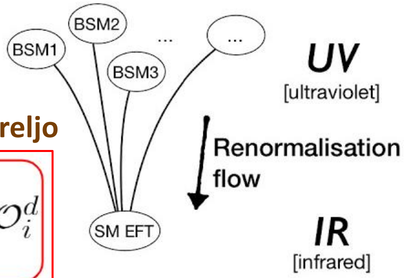

Standard Model Effective Field Theory (SMEFT)

SMEFT is an **EFT which is constructed about the electroweak preserving vacuum**, out of the Higgs doublet Φ which **linearly realises electroweak symmetry breaking**

SMEFT written as Taylor expansion about $\Phi = 0$ in terms of operators increasing in mass dimensions

$$\boxed{\mathcal{L} = \mathcal{L}_{SM}^{d=4} + \sum_{d\geq 5}\sum_{i} \frac{c_i}{\Lambda^{d-4}}\mathcal{O}_i^d}$$

Operators invariant under SM gauge symmetry $SU(3)_C \times SU(2)_L \times U(1)_Y$ and suppressed by powers of new-physics scale, **Λ**

Expanding SMEFT operators show correlations (in broken phase) between different couplings, Higgs multiplicities

Example: $(H^\dagger \sigma_a H) W^a_{\mu\nu} B^{\mu\nu}$ with $\hat{h} = h + v$ gives the following Higgs deformations;
$hA_{\mu\nu}A^{\mu\nu}, hA_{\mu\nu}Z^{\mu\nu}, hZ_{\mu\nu}Z^{\mu\nu}, hW^+_{\mu\nu}W^{-\mu\nu}$, Triple Gauge Couplings $2igc_{\theta_W} W^-_\mu W^+_\nu (A_{\mu\nu} - t_{\theta_W} Z^{\mu\nu})$, S-parameter $\hat{W}_{\mu\nu}B^{\mu\nu}$

Vh production at *pp* colliders

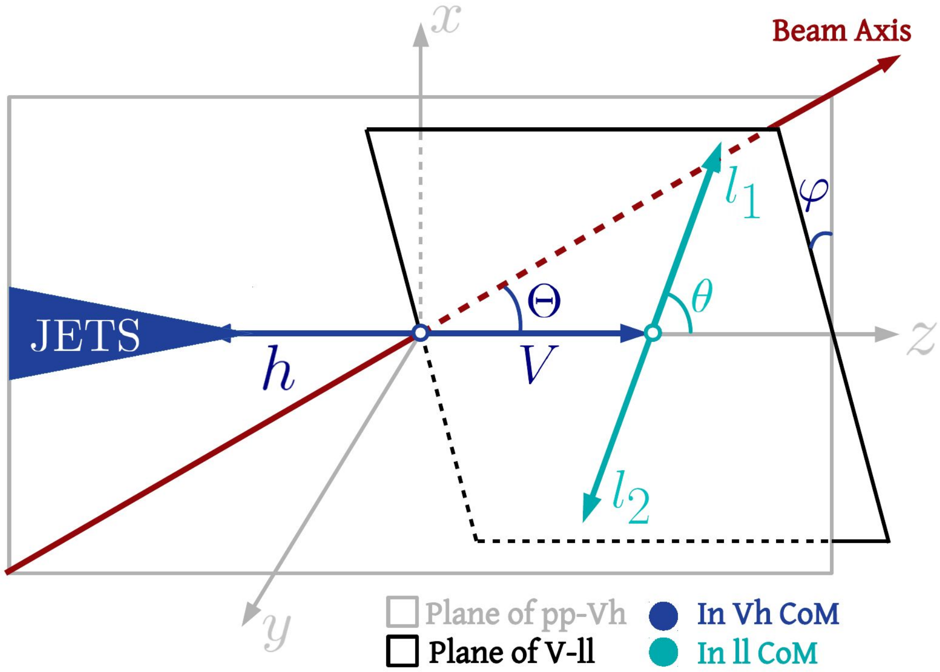

$$Vh\ \left(\frac{d\sigma}{dEd\Theta d\theta d\varphi}\right)$$

Vh production at *pp* colliders

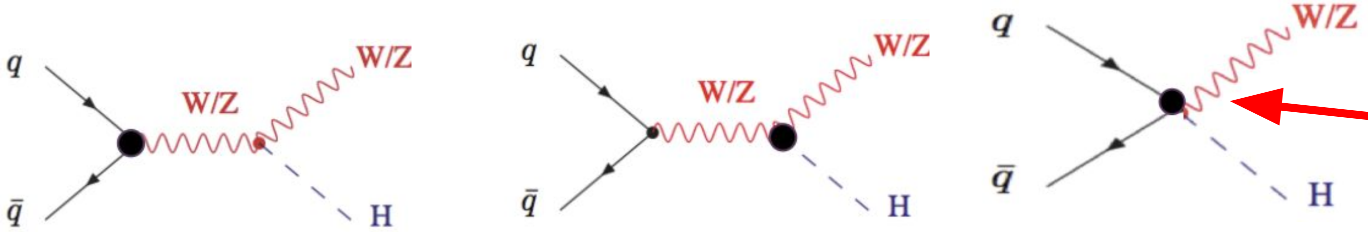

Diagram not there in SM

Can be made more differential!

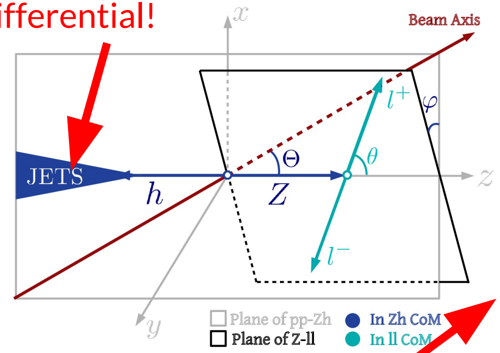

$$
\begin{aligned}
f_{LL} &= S_\Theta^2 S_\theta^2,\\
f_{TT}^1 &= C_\Theta C_\theta,\\
f_{TT}^2 &= (1+C_\Theta^2)(1+C_\theta^2)\\
f_{LT}^1 &= C_\varphi S_\Theta S_\theta,\\
f_{LT}^2 &= C_\varphi S_\Theta S_\theta C_\Theta C_\theta,\\
\tilde{f}_{LT}^1 &= S_\varphi S_\Theta S_\theta,\\
\tilde{f}_{LT}^2 &= S_\varphi S_\Theta S_\theta C_\Theta C_\theta,\\
f_{TT'} &= C_{2\varphi} S_\Theta^2 S_\theta^2,\\
\tilde{f}_{TT'} &= S_{2\varphi} S_\Theta^2 S_\theta^2,
\end{aligned}
$$

Possible to probe multiple angular observables

$\mathcal{O}_{H\Box} = (H^\dagger H)\Box(H^\dagger H)$	$\mathcal{O}_{HL}^{(3)} = iH^\dagger \sigma^a \overleftrightarrow{D}_\mu H \bar{L}\sigma^a\gamma^\mu L$
$\mathcal{O}_{HD} = (H^\dagger D_\mu H)^*(H^\dagger D_\mu H)$	$\mathcal{O}_{HB} = \lvert H\rvert^2 B_{\mu\nu}B^{\mu\nu}$
$\mathcal{O}_{Hu} = iH^\dagger \overleftrightarrow{D}_\mu H \bar{u}_R\gamma^\mu u_R$	$\mathcal{O}_{HWB} = H^\dagger\sigma^a H W^a_{\mu\nu}B^{\mu\nu}$
$\mathcal{O}_{Hd} = iH^\dagger \overleftrightarrow{D}_\mu H \bar{d}_R\gamma^\mu d_R$	$\mathcal{O}_{HW} = \lvert H\rvert^2 W_{\mu\nu}W^{\mu\nu}$
$\mathcal{O}_{He} = iH^\dagger \overleftrightarrow{D}_\mu H \bar{e}_R\gamma^\mu e_R$	$\mathcal{O}_{H\tilde{B}} = \lvert H\rvert^2 B_{\mu\nu}\tilde{B}^{\mu\nu}$
$\mathcal{O}_{HQ}^{(1)} = iH^\dagger \overleftrightarrow{D}_\mu H \bar{Q}\gamma^\mu Q$	$\mathcal{O}_{H\tilde{W}B} = H^\dagger\sigma^a H W^a_{\mu\nu}\tilde{B}^{\mu\nu}$
$\mathcal{O}_{HQ}^{(3)} = iH^\dagger\sigma^a \overleftrightarrow{D}_\mu H \bar{Q}\sigma^a\gamma^\mu Q$	$\mathcal{O}_{H\tilde{W}} = \lvert H\rvert^2 W^a_{\mu\nu}\tilde{W}^{a\mu\nu}$
$\mathcal{O}_{HL}^{(1)} = iH^\dagger \overleftrightarrow{D}_\mu H \bar{L}\gamma^\mu L$	$\mathcal{O}_{y_b} = y_b\lvert H\rvert^2(\bar{Q}Hb_R + h.c).$

CP-odd operators

D6 operators in Warsaw basis contributing to anomalous hVV*/hVff couplings

Zh production (Helicity amplitude)

- For a $2 \to 2$ process $f(\sigma)\bar{f}(-\sigma) \to Zh$, the helicity amplitudes are given by

$$\mathcal{M}_\sigma^{\lambda=\pm} = \sigma \frac{1+\sigma\lambda\cos\Theta}{\sqrt{2}} G_V \frac{m_V}{\boxed{\sqrt{\hat{s}}}} \left[\boxed{1} + \left(\frac{g_{Vf}^h}{g_f^V} + \hat{\kappa}_{VV} - i\lambda\hat{\tilde{\kappa}}_{VV} \right) \frac{\hat{s}}{2m_V^2} \right]$$

$$\mathcal{M}_\sigma^{\lambda=0} = -\frac{\sin\Theta}{2} G_V \left[\boxed{1} + \delta\hat{g}_{VV}^h + 2\hat{\kappa}_{VV} + \delta g_f^Z + \frac{g_{Vf}^h}{g_f^V} \left(-\frac{1}{2} + \frac{\hat{s}}{2m_V^2} \right) \right]$$

$$\begin{aligned} \hat{\kappa}_{WW} &= \kappa_{WW} \\ \hat{\kappa}_{ZZ} &= \kappa_{ZZ} + \frac{Q_f e}{g_f^Z} \kappa_{Z\gamma}, \\ \hat{\tilde{\kappa}}_{ZZ} &= \tilde{\kappa}_{ZZ} + \frac{Q_f e}{g_f^Z} \tilde{\kappa}_{Z\gamma} \end{aligned}$$

- $\lambda = \pm 1$ and $\sigma = \pm 1$ are, respectively, the helicities of the Z-boson and initial-state fermions, $g_f^Z = g(T_3^f - Q_f s_{\theta_W}^2)/c_{\theta_W}$
- Leading SM is longitudinal ($\lambda = 0$), Leading effect of $\kappa_{WW}, \kappa_{ZZ}, \tilde{\kappa}_{ZZ}$ is in the transverse-longitudinal (LT) interference, LT term vanishes if we aren't careful

Angular observables: *Zh* and *Wh* production at the LHC

$$\epsilon_{LR} = \frac{(g_{l_R}^V)^2 - (g_{l_L}^V)^2}{(g_{l_R}^V)^2 + (g_{l_L}^V)^2} \qquad \mathcal{G} = g g_f^Z \sqrt{(g_{l_L}^Z)^2 + (g_{l_R}^Z)^2} / (\cos\theta_W \Gamma_Z) \qquad \gamma = \sqrt{\hat{s}}/(2 m_V)$$

$$\begin{aligned}
\sum_{L,R} |\mathcal{A}(\hat{s}, \Theta, \theta, \varphi)|^2 &= a_{LL} \sin^2\Theta \sin^2\theta + a_{TT}^1 \cos\Theta \cos\theta \\
&+ a_{TT}^2 (1 + \cos^2\Theta)(1 + \cos^2\theta) + \cos\varphi \sin\Theta \sin\theta \\
&\times (a_{LT}^1 + a_{LT}^2 \cos\theta \cos\Theta) + \sin\varphi \sin\Theta \sin\theta \\
&\times (\tilde{a}_{LT}^1 + \tilde{a}_{LT}^2 \cos\theta \cos\Theta) + a_{TT'} \cos 2\varphi \sin^2\Theta \sin^2\theta \\
&+ \tilde{a}_{TT'} \sin 2\varphi \sin^2\Theta \sin^2\theta
\end{aligned}$$

a_{LL}	$\frac{\mathcal{G}^2}{4}\left[1 + 2\delta\hat{g}_{VV}^h + 4\hat{\kappa}_{VV} + 2\delta g_f^Z + \frac{g_{Vf}^h}{g_f^V}(-1 + 4\gamma^2)\right]$
a_{TT}^1	$\frac{\mathcal{G}^2 \sigma \epsilon_{RL}}{2\gamma^2}\left[1 + 4\left(\frac{g_{Vf}^h}{g_f^V} + \hat{\kappa}_{VV}\right)\gamma^2\right]$
a_{TT}^2	$\frac{\mathcal{G}^2}{8\gamma^2}\left[1 + 4\left(\frac{g_{Vf}^h}{g_f^V} + \hat{\kappa}_{VV}\right)\gamma^2\right]$
a_{LT}^1	$-\frac{\mathcal{G}^2 \sigma \epsilon_{RL}}{2\gamma}\left[1 + 2\left(\frac{2g_{Vf}^h}{g_f^V} + \hat{\kappa}_{VV}\right)\gamma^2\right]$
a_{LT}^2	$-\frac{\mathcal{G}^2}{2\gamma}\left[1 + 2\left(\frac{2g_{Vf}^h}{g_f^V} + \hat{\kappa}_{VV}\right)\gamma^2\right]$
$\tilde{a}_{LT}^1$	$-\mathcal{G}^2 \sigma \epsilon_{RL} \hat{\tilde{\kappa}}_{VV} \gamma$
$\tilde{a}_{LT}^2$	$-\mathcal{G}^2 \hat{\tilde{\kappa}}_{VV} \gamma$
$a_{TT'}$	$\frac{\mathcal{G}^2}{8\gamma^2}\left[1 + 4\left(\frac{g_{Vf}^h}{g_f^V} + \kappa\hat{V}V\right)\gamma^2\right]$
$\tilde{a}_{TT'}$	$\frac{\mathcal{G}^2}{2}\hat{\tilde{\kappa}}_{VV}$

Suppressed moments

Vh production at *pp* colliders

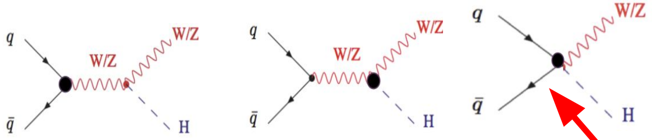

Diagram not in the SM

SM scaling κ-framework

$$
\begin{aligned}
\Delta\mathcal{L}_6 \supset\; & \delta\hat{g}^h_{WW}\,\frac{2m_W^2}{v}\,hW^{+\mu}W^-_\mu + \boxed{\delta\hat{g}^h_{ZZ}\,\frac{2m_Z^2}{v}\,h\frac{Z^\mu Z_\mu}{2}} + \delta g^W_Q\,(W^+_\mu \bar{u}_L\gamma^\mu d_L + h.c.)\\
&+ \delta g^W_L\,(W^+_\mu \bar{\nu}_L\gamma^\mu e_L + h.c.) + g^h_{WL}\,\frac{h}{v}(W^+_\mu \bar{\nu}_L\gamma^\mu e_L + h.c.)\\
&+ g^h_{WQ}\,\frac{h}{v}(W^+_\mu \bar{u}_L\gamma^\mu d_L + h.c.) + \sum_f \delta g^Z_f Z_\mu \bar{f}\gamma^\mu f + \boxed{\sum_f g^h_{Zf}\,\frac{h}{v}Z_\mu \bar{f}\gamma^\mu f}\\
&+ \kappa_{WW}\,\frac{h}{v}W^{+\mu\nu}W^-_{\mu\nu} + \tilde{\kappa}_{WW}\,\frac{h}{v}W^{+\mu\nu}\tilde{W}^-_{\mu\nu} + \boxed{\kappa_{ZZ}\,\frac{h}{2v}Z^{\mu\nu}Z_{\mu\nu}}\\
&+ \boxed{\tilde{\kappa}_{ZZ}\,\frac{h}{2v}Z^{\mu\nu}\tilde{Z}_{\mu\nu}} + \kappa_{Z\gamma}\,\frac{h}{v}A^{\mu\nu}Z_{\mu\nu} + \tilde{\kappa}_{Z\gamma}\,\frac{h}{v}A^{\mu\nu}\tilde{Z}_{\mu\nu} + \delta\hat{g}^h_{bb}\,\frac{\sqrt{2}m_b}{v}\,hb\bar{b}\\
&+ \kappa_{\gamma\gamma}\,\frac{h}{v}A^{\mu\nu}A_{\mu\nu}
\end{aligned}
$$

4 directions relevant for the high-energy primaries (to follow) $\delta g^Z_{u_R}, \delta g^Z_{d_R}, \delta g^Z_{u_L}, \delta g^Z_{d_L}$

Contact interaction; no propagator; Energy growth

CP-even new Lorentz structure (angular deformation)

CP-odd new Lorentz structure (angular deformation)

Deformations written in broken phase after symmetry breaking

High-energy primaries

1. **The four channels, *viz.*, Zh, $W^{\pm}h$, $W^{+}W^{-}$ and $W^{\pm}Z$ can be expressed (at high energies) respectively as $G^{0}h$, $G^{\pm}h$, $G^{+}G^{-}$ and $G^{\pm}G^{0}$ and the Higgs field can be written as**

$$\begin{pmatrix} G^{+} \\ \frac{h+iG^{0}}{2} \end{pmatrix}$$

2. **These four final states are intrinsically connected by gauge symmetry even though they are very different from a collider physics point of view**

3. **With the Goldstone boson equivalence theorem, it is possible to compute amplitudes for various components of the Higgs in the unbroken phase**

4. **Full *SU(2)* theory is manifest [Franceschini, Panico, Pomarol, Riva, Wulzer, 2017]**

High-energy primaries

Amplitude	High-energy primaries
$\bar{u}_L d_L \to W_L Z_L, W_L h$	$\sqrt{2} a_q^{(3)}$
$\bar{u}_L u_L \to W_L W_L$ $\bar{d}_L d_L \to Z_L h$	$a_q^{(1)} + a_q^{(3)}$
$\bar{d}_L d_L \to W_L W_L$ $\bar{u}_L u_L \to Z_L h$	$a_q^{(1)} - a_q^{(3)}$
$\bar{f}_R f_R \to W_L W_L, Z_L h$	a_f

Amplitude	High-energy primaries	Low-energy primaries
$\bar{u}_L d_L \to W_L Z_L, W_L h$	$\frac{g^h_{Zd_Ld_L} - g^h_{Zu_Lu_L}}{\sqrt{2}}$	$\sqrt{2}\frac{g^2}{m_W^2}\left[c_{\theta_W}(\delta g^Z_{uL} - \delta g^Z_{dL})/g - c^2_{\theta_W}\delta g_1^Z\right]$
$\bar{u}_L u_L \to W_L W_L$ $\bar{d}_L d_L \to Z_L h$	$g^h_{Zd_Ld_L}$	$-\frac{2g^2}{m_W^2}\left[Y_L t^2_{\theta_W}\delta\kappa_\gamma + T_Z^{u_L}\delta g_1^Z + c_{\theta_W}\delta g^Z_{dL}/g\right]$
$\bar{d}_L d_L \to W_L W_L$ $\bar{u}_L u_L \to Z_L h$	$g^h_{Zu_Lu_L}$	$-\frac{2g^2}{m_W^2}\left[Y_L t^2_{\theta_W}\delta\kappa_\gamma + T_Z^{d_L}\delta g_1^Z + c_{\theta_W}\delta g^Z_{uL}/g\right]$
$\bar{f}_R f_R \to W_L W_L, Z_L h$	$g^h_{Zf_Rf_R}$	$-\frac{2g^2}{m_W^2}\left[Y_{f_R} t^2_{\theta_W}\delta\kappa_\gamma + T_Z^{f_R}\delta g_1^Z + c_{\theta_W}\delta g^Z_{fR}/g\right]$

***Vh* and *VV* channels are entwined by symmetry and they constrain the same set of observables at High energies but may have different directions [Franceschini, Panico,Pomarol, Riva, Wulzer, 2017, SB, Gupta, Seth, Reiness, Spannowsky, 2020]**

High-energy primaries

SILH basis	Warsaw basis
$\mathcal{O}_W = \frac{ig}{2}(H^\dagger \sigma^a \overleftrightarrow{D}^\mu H) D^\nu W^a_{\mu\nu}$	$\mathcal{O}_L^{(3)} = (\bar{Q}_L \sigma^a \gamma^\mu Q_L)(iH^\dagger \sigma^a \overleftrightarrow{D}_\mu H)$
$\mathcal{O}_B = \frac{ig'}{2}(H^\dagger \overleftrightarrow{D}^\mu H) \partial^\nu B^a_{\mu\nu}$	$\mathcal{O}_L = (\bar{Q}_L \gamma^\mu Q_L)(iH^\dagger \overleftrightarrow{D}_\mu H)$
$\mathcal{O}_{HW} = ig(D^\mu H)^\dagger \sigma^a (D^\nu H) W^a_{\mu\nu}$	$\mathcal{O}_R^u = (\bar{u}_R \gamma^\mu u_R)(iH^\dagger \overleftrightarrow{D}_\mu H)$
$\mathcal{O}_{HB} = ig(D^\mu H)^\dagger (D^\nu H) B_{\mu\nu}$	$\mathcal{O}_R^d = (\bar{d}_R \gamma^\mu d_R)(iH^\dagger \overleftrightarrow{D}_\mu H)$
$\mathcal{O}_{2W} = -\frac{1}{2}(D^\mu W^a_{\mu\nu})^2$	
$\mathcal{O}_{2B} = -\frac{1}{2}(\partial^\mu B_{\mu\nu})^2$	

Dimension-6 operators contributing to the high energy longitudinal diboson production channels in the SILH and Warsaw bases [Franceschini, Panico,Pomarol, Riva, Wulzer, 2017]

$$a_u = 4\frac{c_R^u}{\Lambda^2}, a_d = 4\frac{c_R^d}{\Lambda^2}, a_q^{(1)} = 4\frac{c_L^{(1)}}{\Lambda^2}, \text{ and } a_q^{(3)} = 4\frac{c_L^{(3)}}{\Lambda^2}$$

Relating the high-energy primaries with the Warsaw basis operators

We are dealing with four channels and there are only four independent couplings at play at high energies.

Vh production at *pp* colliders

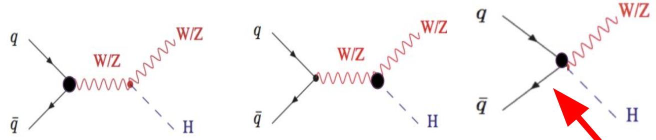

Diagram not in the SM

SM scaling
κ-framework

$$
\begin{aligned}
\Delta\mathcal{L}_6 \supset\; & \delta\hat{g}^h_{WW}\,\frac{2m_W^2}{v}\,hW^{+\mu}W^-_\mu + \boxed{\delta\hat{g}^h_{ZZ}\,\frac{2m_Z^2}{v}\,h\frac{Z^\mu Z_\mu}{2}} + \delta g^W_Q\,(W^+_\mu\bar{u}_L\gamma^\mu d_L + h.c.)\\
+\; & \delta g^W_L\,(W^+_\mu\bar{\nu}_L\gamma^\mu e_L + h.c.) + g^h_{WL}\,\frac{h}{v}(W^+_\mu\bar{\nu}_L\gamma^\mu e_L + h.c.)\\
+\; & g^h_{WQ}\,\frac{h}{v}(W^+_\mu\bar{u}_L\gamma^\mu d_L + h.c.) + \sum_f \delta g^Z_f Z_\mu\bar{f}\gamma^\mu f + \boxed{\sum_f g^h_{Zf}\,\frac{h}{v}Z_\mu\bar{f}\gamma^\mu f}\\
+\; & \kappa_{WW}\,\frac{h}{v}W^{+\mu\nu}W^-_{\mu\nu} + \tilde{\kappa}_{WW}\,\frac{h}{v}W^{+\mu\nu}\tilde{W}^-_{\mu\nu} + \boxed{\kappa_{ZZ}\,\frac{h}{2v}Z^{\mu\nu}Z_{\mu\nu}}\\
+\; & \boxed{\tilde{\kappa}_{ZZ}\,\frac{h}{2v}Z^{\mu\nu}\tilde{Z}_{\mu\nu}} + \kappa_{Z\gamma}\,\frac{h}{v}A^{\mu\nu}Z_{\mu\nu} + \tilde{\kappa}_{Z\gamma}\,\frac{h}{v}A^{\mu\nu}\tilde{Z}_{\mu\nu} + \delta\hat{g}^h_{bb}\,\frac{\sqrt{2}m_b}{v}\,hb\bar{b}\\
+\; & \kappa_{\gamma\gamma}\,\frac{h}{v}A^{\mu\nu}A_{\mu\nu}
\end{aligned}
$$

4 directions relevant for the high-energy primaries (to follow) $\delta g^Z_{u_R}, \delta g^Z_{d_R}, \delta g^Z_{u_L}, \delta g^Z_{d_L}$

Contact interaction; no propagator; Energy growth

CP-even new Lorentz structure (angular deformation)

CP-odd new Lorentz structure (angular deformation)

Deformations written in broken phase after symmetry breaking

Differential in energy: constraining the contact terms

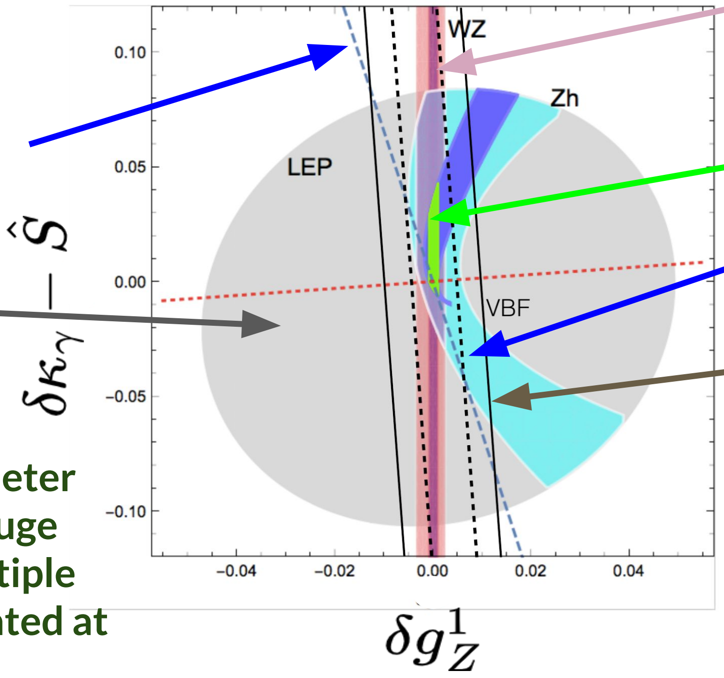

Exclusion from *WZ* [Franceschini et al, 2017]

Zh + *WZ* combined

Exclusion from *Zh* [SB, Englert, Gupta, Spannowsky, 2018]

WBF analysis in diphoton channel [Araz, SB, Gupta, Spannowsky, 2020]

What about WW?

Accidental cancellation of interference terms

LEP exclusion region

A common parameter space in triple-gauge couplings for multiple channels - correlated at high energies

Differential in angles: constraining the angular terms

- Method of moments used to constrain the other couplings
- We obtain **percent level bounds on κ_{ZZ} and in the $(\kappa_{ZZ}, \delta\hat{g}^h_{ZZ})$ plane**
- Competitive and complementary bounds to previous analyses
- Independent bound on the *CP*-odd coupling, $\boxed{|\tilde{\kappa}^p_{ZZ}| < 0.03}$

CP-odd couplings!

- We obtain **percent level bounds on κ_{WW} and in the $(\kappa_{WW}, \delta\hat{g}^h_{WW})$ plane**
- Competitive and complementary bounds to previous analyses
- Independent bound on the *CP*-odd coupling, $\boxed{|\tilde{\kappa}^p_{WW}| < 0.04}$

$$\tilde{\kappa}_{WW} = \frac{2v^2}{\Lambda^2} c_{H\tilde{W}}$$

$$\tilde{\kappa}_{ZZ} = \frac{2v^2}{\Lambda^2}(\cos^2\theta_W c_{H\tilde{W}} + \sin^2\theta_W c_{H\tilde{B}} + sin\theta_W cos\theta_W c_{H\tilde{W}B})$$

Assuming Λ = 1 TeV, $c_{H\tilde{W}} < 0.33$ at 68% C.L. at HL-LHC!

We consider all operators simultaneously!
ATLAS considers one at a time

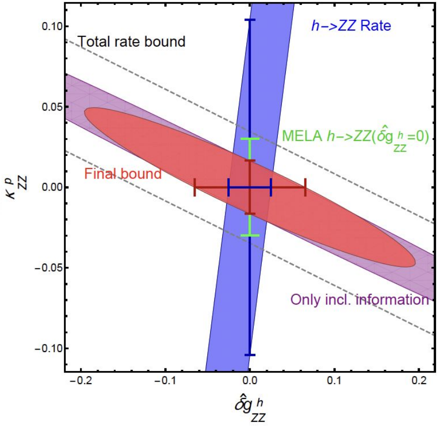

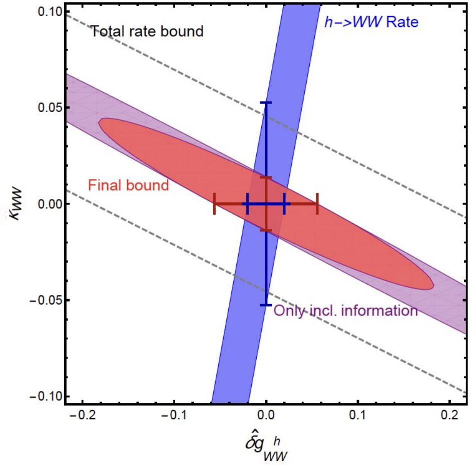

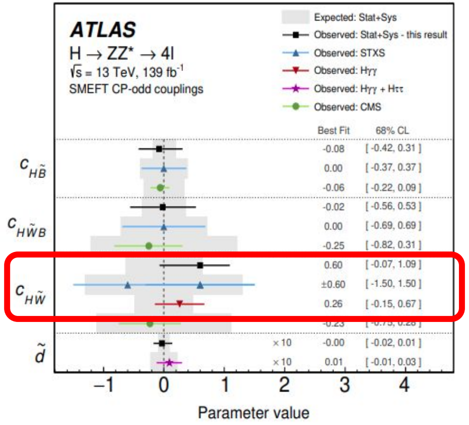

Theory uncertainties in EFT analyses: NLO effects (QCD)

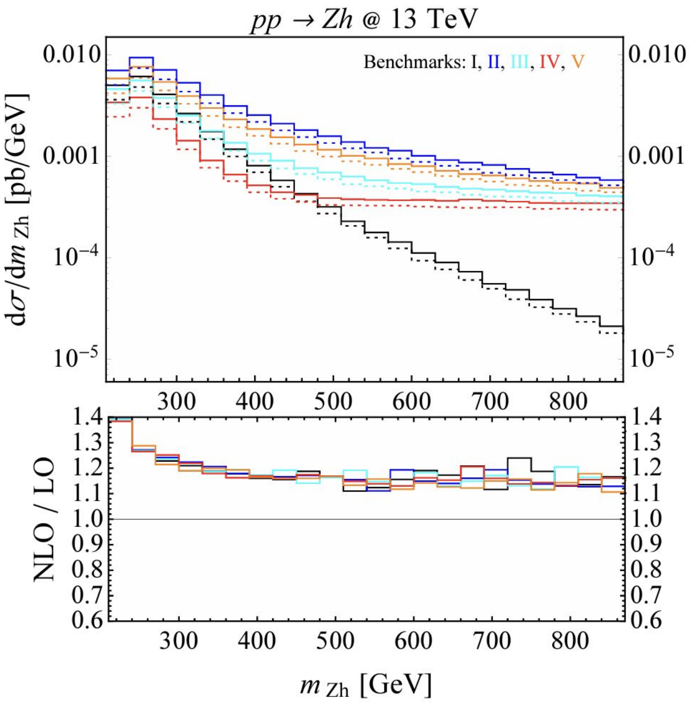

Automated in MG5_aMC@NLO through NLOCT!

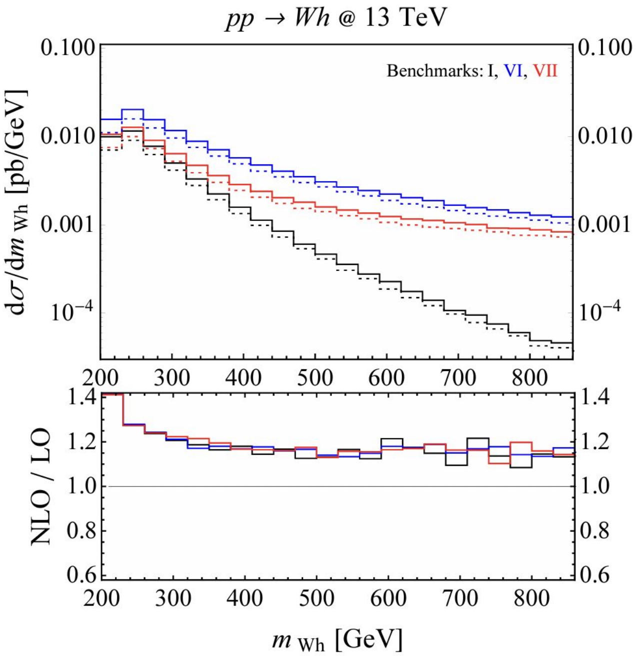

Greljo et al, 2017

Electroweak corrections

We include approximate electroweak (EW) corrections in Sherpa which includes infrared subtracted EW 1-loop corrections as additional weights to the respective Born cross sections. In those the event weight is calculated based on the expression

$$\mathrm{d}\sigma_{\mathrm{NLO,EW}_{\mathrm{approx}}} = \left[B(\Phi) + V_{\mathrm{EW}}(\Phi) + I_{\mathrm{EW}}(\Phi)\right]\mathrm{d}\Phi$$

B = Born contribution also entering the uncorrected QCD cross Section

V_{EW} = electroweak virtual corrections at 1-loop accuracy

I_{EW} = generalised Catani-Seymour insertion operator for EW NLO calculations.

Latter subtracts all infrared singularities of the virtual corrections. This fundamentally arbitrary procedure should provide a good approximation if electroweak Sudakov logarithms are dominant.

The W^+W^- channel

$$
\begin{aligned}
\Delta\mathcal{L}_{\mathrm{BSM}} = {} & \delta g^Z_{uL}\left[Z^\mu \bar{u}_L\gamma_\mu u_L + \frac{\cos\theta_W}{\sqrt{2}}\left(W^{+\mu}\bar{u}_L\gamma_\mu d_L + \mathrm{h.c.}\right) + \ldots\right] + \delta g^Z_{uR}\left[Z^\mu \bar{u}_R\gamma_\mu u_R\right] \\
& + \delta g^Z_{dL}\left[Z^\mu \bar{d}_L\gamma_\mu d_L - \frac{\cos\theta_W}{\sqrt{2}}\left(W^{+\mu}\bar{u}_L\gamma_\mu d_L + \mathrm{h.c.}\right) + \ldots\right] + \delta g^Z_{dR}\left[Z^\mu \bar{d}_R\gamma_\mu d_R\right] \\
& + ig\cos\theta_W \delta g^Z_1\left[Z^\mu\left(W^{+\nu}W^-_{\mu\nu} - \mathrm{h.c.}\right) + Z^{\mu\nu}W^+_\mu W^-_\nu + \ldots\right] \\
& + ie\delta\kappa_\gamma\left[\left(A_{\mu\nu} - \tan\theta_W Z_{\mu\nu}\right)W^{+\mu}W^{-\nu} + \ldots\right],
\end{aligned}
$$

with $Z_{\mu\nu} \equiv \hat{Z}_{\mu\nu} - iW^+_{[\mu}W^-_{\nu]}$, $A_{\mu\nu} \equiv \hat{A}_{\mu\nu}$, $W^\pm_{\mu\nu} \equiv \hat{W}^\pm_{\mu\nu} \pm iW^\pm_{[\mu}(A+Z)_{\nu]}$, where $\hat{V}_{\mu\nu} = \partial_\mu V_\nu - \partial_\nu V_\mu$, and θ_W is the Weinberg angle

Electroweak corrections in W^+W^-

Leading order

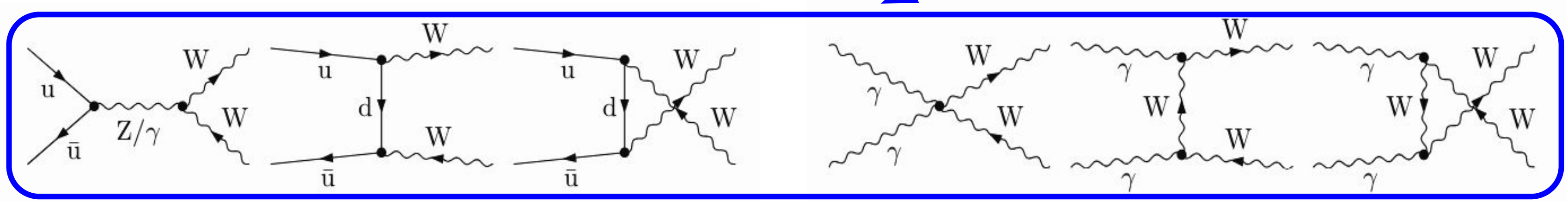

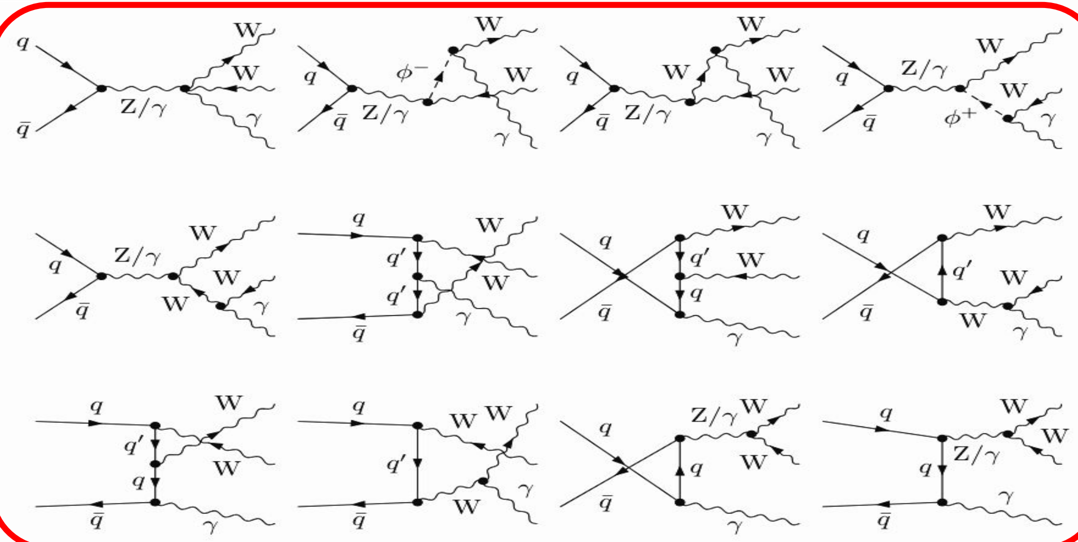

[Bierweiler et al, 2012]

Real bremsstrahlung diagrams

Electroweak corrections in W^+W^-

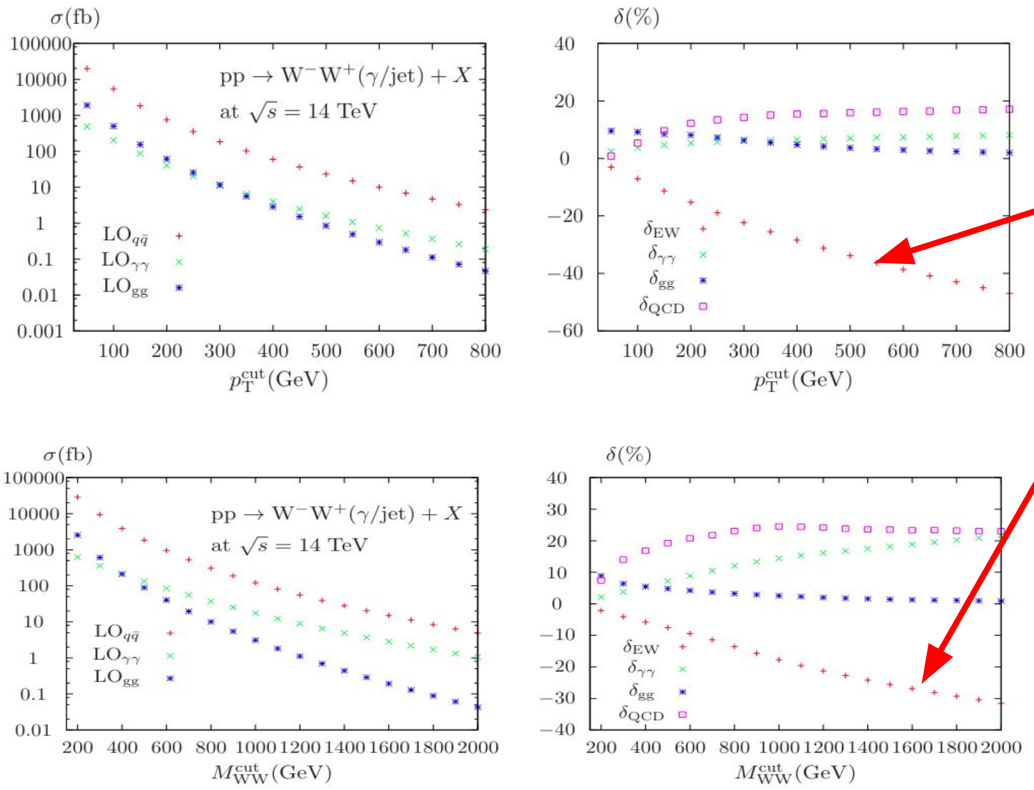

Large (negative) electroweak corrections!

[arXiv:1208.3147: Bierweiler, Kasprzik, Kühn, Uccirati]

Electroweak corrections in *W⁺W⁻(+jj)*

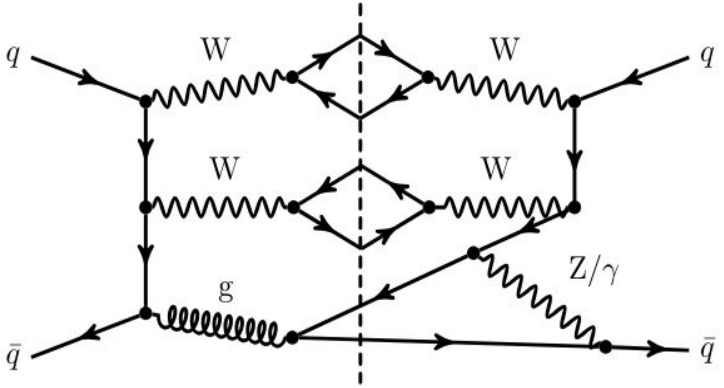

Squared sample diagram representing interference contributions in the real corrections at order $\mathcal{O}(\alpha_s\alpha^5)$ in the channel $pp \to \mu^+\nu_\mu e^-\bar{\nu}_e jj$.

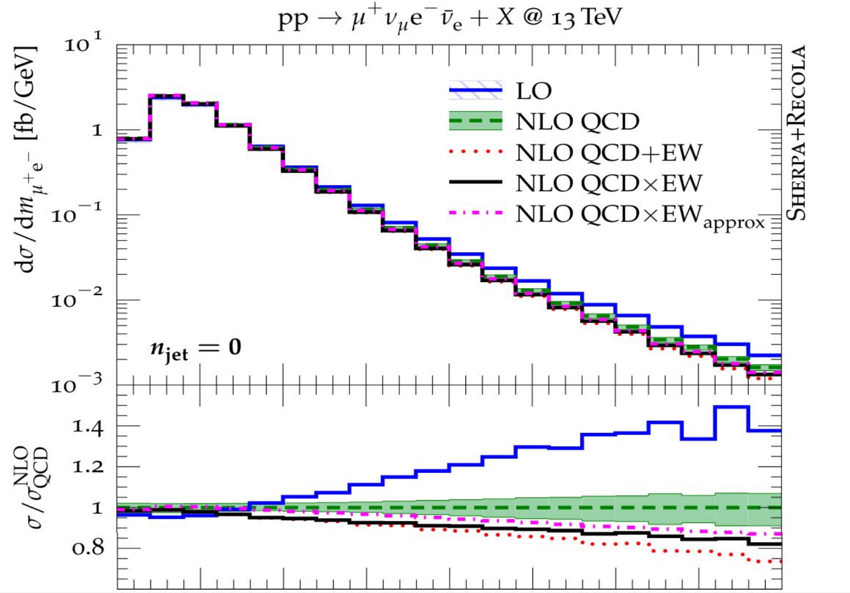

[arXiv:2005.12128: Bräuer, Denner, Pellen, Schönherr, Schumann, 2020]

Comparing full QCD x EW corrections with QCD x EW (approx.)

Event generation

$$pp \to W^+(l^+\nu)W^-(l^-\nu)$$

$$\mu_R^2 = \mu_F^2 = M^2_{\perp,W^+} + M^2_{\perp,W^-}$$

[SB, Reichelt, Spannowsky, 2024]

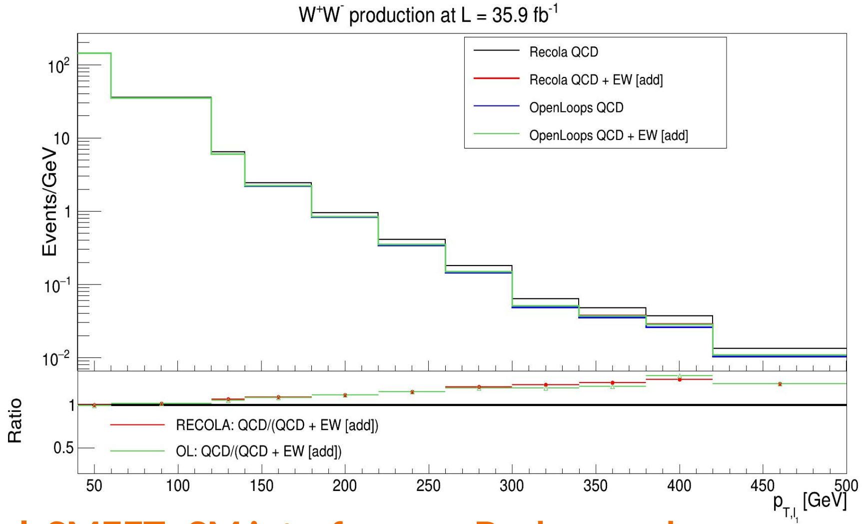

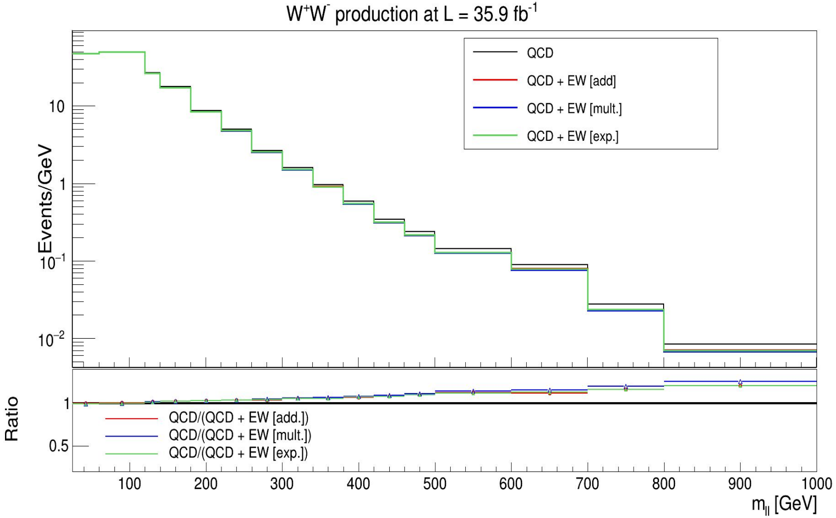

Signal: SMEFT+SM interference; Backgrounds: Drell-Yan $(pp \to \ell^+\ell^-), VZ, t\bar{t} + tW, W\ell\ell$

The ME W^+W^-Z is significantly suppressed because of phase-space. Moreover, the CMS analysis that is used here reduces this background even further. There are 12 VVV events when compared to ~6500 qq → W^+W^- events at 36 fb^{-1}.

χ^2 analysis

EFT coupling

$$\mathcal{O}_{ij}^{\text{theo.}}(p) = \mathcal{O}_{ij}^{\text{SM}} + p \times \mathcal{O}_{ij}^{\text{SMEFT}}$$

Our signal is the interference between SM and SMEFT

$$\chi^2 = \sum_i \sum_j \frac{[\mathcal{O}_{ij}^{\text{theo.}}(p) - \mathcal{O}_{ij}^{\text{exp., SM}}]^2}{\sigma_{ij}^2}$$

$$p = \delta g_{d_R}^Z, \delta g_{u_R}^Z, \delta g_{u_L}^Z, \text{ or } \delta g_{d_L}^Z$$

$$\sigma_{ij} = \sqrt{(\sigma_{ij,\text{stat.}}^{\text{exp.}})^2 + (\sigma_{ij,\text{stat.}}^{\text{theo.}})^2 + (\sigma_{ij,\text{syst.}}^{\text{exp.}})^2 + (\sigma_{ij,\text{syst.}}^{\text{theo.}})^2}$$

6 sub-categories: $e\mu - 0, e\mu - 1, ee - 0, ee - 1, \mu\mu - 0,$ and $\mu\mu - 1$
`0' and `1' refer to the jet multiplicity

Theo. calculated at either SM@NLO-QCD+approximate-NLO-EW + SMEFT@LO or SM@NLO-QCD + SMEFT@LO

Exp. calculated at SM@NLO-QCD+approximate-NLO-EW

Results (95% C.L. bounds) - 1 and 2 parameter fits

[SB, Reichelt, Spannowsky, 2024]

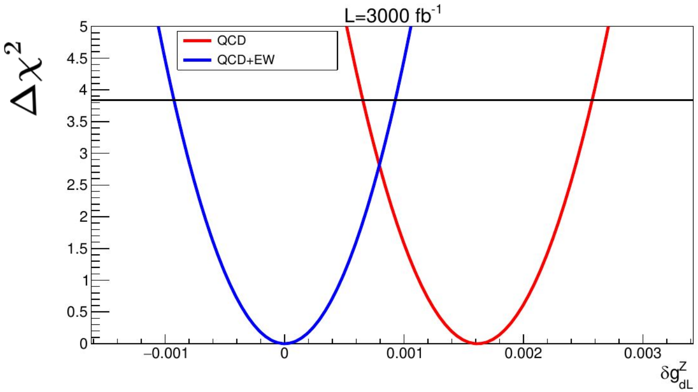

Big difference between red and blue regions!

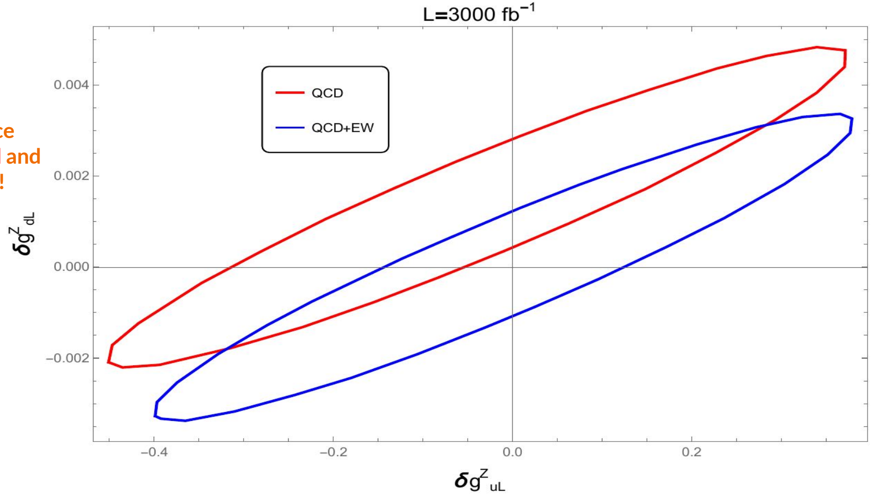

Coupling	QCD: $\mathcal{L} = 300$ fb^{-1}	QCD+EW: $\mathcal{L} = 300$ fb^{-1}	QCD: $\mathcal{L} = 3$ ab^{-1}	QCD+EW: $\mathcal{L} = 3$ ab^{-1}
$\delta g^Z_{d_R}$	[-0.2744 0.0531]	[-0.1569, 0.1569]	[-0.1611, -0.0421]	[-0.0567, 0.0567]
$\delta g^Z_{u_R}$	[-0.0180, 0.0818]	[-0.0474, 0.0474]	[0.0111, 0.0463]	[-0.0167, 0.0167]
$\delta g^Z_{d_L}$	[-0.0008, 0.0039]	[-0.0023, 0.0023]	[0.0006, 0.0026]	[-0.0010, 0.0010]
$\delta g^Z_{u_L}$	[-0.3910, 0.0927]	[-0.2383, 0.2383]	[-0.2969, -0.0702]	[-0.1104, 0.1104]

Summary

1. EFTs are important tools to understand the possible nature and type of new physics when resonance searches are not yielding results.

2. *Zh*, *Wh*, *WW* and *WZ* are important channels to disentangle various directions in the EFT space. They are intrinsically correlated.

3. Multiple dimensions come about from the various correlated EFT coefficients. Blind directions need to be broken.

4. Inclusion of electroweak corrections to the backgrounds can change the bounds on the SMEFT couplings considerably as what we may perceive to be a change owing to SMEFT deformations might be owing to higher-order corrections. What about corrections to the SMEFT part?

5. Various sources of theory uncertainties need to be understood and incorporated in analyses. These include uncertainties from operator truncation, NLO QCD effects, NLO EW effects, RGE effects, and more.

Backup slides

EFT in particle physics: Motivation

LHC has not yet found conclusive evidence of any BSM physics

Two broad methodologies to search for new physics:

Model dependent: Study signatures of a (preferably UV-complete) model carefully
"Model independent": Parametrise our ignorance as a low energy effective theory formalism

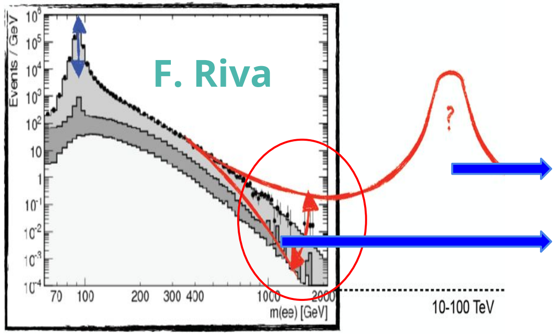

SM (or any BSM theory) → low energy effective theory valid below a cut-off scale Λ. EFT → choosing a set of low-energy DOF, specifying UV cut-off and symmetries

Bigger theory assumed to supersede low-energy model above Λ

EFT effects can manifest as deformation in angular distributions, excess events in high-energy tails, etc. → Extreme precision in theoretical understanding needed!!!

At perturbative level, heavy (> Λ) DOF decoupled from low-energy theory

Vh production at *pp* colliders

$$
\begin{aligned}
f_{LL} &= S_\Theta^2 S_\theta^2,\\
f_{TT}^1 &= C_\Theta C_\theta,\\
f_{TT}^2 &= (1+C_\Theta^2)(1+C_\theta^2),\\
f_{LT}^1 &= C_\varphi S_\Theta S_\theta,\\
f_{LT}^2 &= C_\varphi S_\Theta S_\theta C_\Theta C_\theta,\\
\tilde{f}_{LT}^1 &= S_\varphi S_\Theta S_\theta,\\
\tilde{f}_{LT}^2 &= S_\varphi S_\Theta S_\theta C_\Theta C_\theta,\\
f_{TT'} &= C_{2\varphi} S_\Theta^2 S_\theta^2,\\
\tilde{f}_{TT'} &= S_{2\varphi} S_\Theta^2 S_\theta^2,
\end{aligned}
$$

Many angular distributions testable at the LHC

- φ, Θ and $\{x, y, z\}$ in *Vh* CoM frame (z identified as direction of V-boson; y identified as normal to the plane of V and beam axis; x defined to complete the right-handed set), θ in V CoM frame
- Q: How much differential information can one extract from this process?
- For three body phase space, $3 \times 3 - 4 = 5$ kinematic variables completely define final state
- Barring boost factor, the variables are $\sqrt{s}, \Theta, \theta, \varphi$

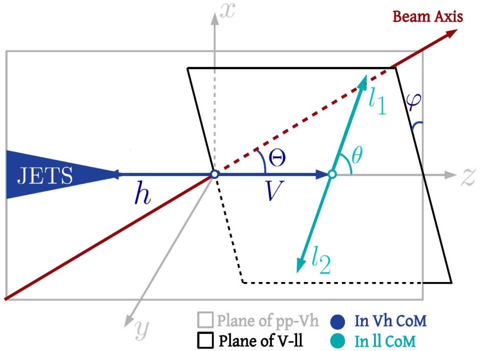

Angular observables: $Vh \longrightarrow 2lbb$ and $ggF\ (h \longrightarrow ZZ^* \longrightarrow 4l)$

$Vh\ \left(\frac{d\sigma}{dEd\Theta d\theta d\varphi}\right)$

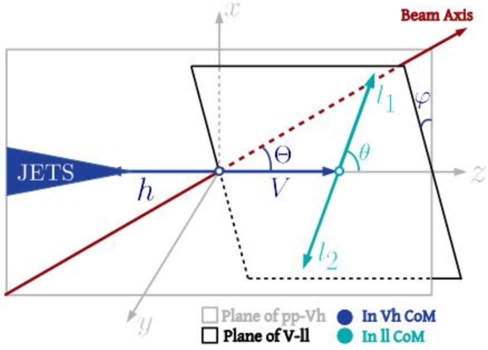

$$
\begin{aligned}
f_{LL} &= S_\Theta^2 S_\theta^2,\\
f_{TT}^1 &= C_\Theta C_\theta,\\
f_{TT}^2 &= (1+C_\Theta^2)(1+C_\theta^2),\\
f_{LT}^1 &= C_\varphi S_\Theta S_\theta,\\
f_{LT}^2 &= C_\varphi S_\Theta S_\theta C_\Theta C_\theta,\\
\tilde{f}_{LT}^1 &= S_\varphi S_\Theta S_\theta,\\
\tilde{f}_{LT}^2 &= S_\varphi S_\Theta S_\theta C_\Theta C_\theta,\\
f_{TT'} &= C_{2\varphi} S_\Theta^2 S_\theta^2,\\
\tilde{f}_{TT'} &= S_{2\varphi} S_\Theta^2 S_\theta^2\,,
\end{aligned}
$$

$ggF\ \left(\frac{d\sigma}{dEd\theta_1 d\theta_2 d\phi}\right)$

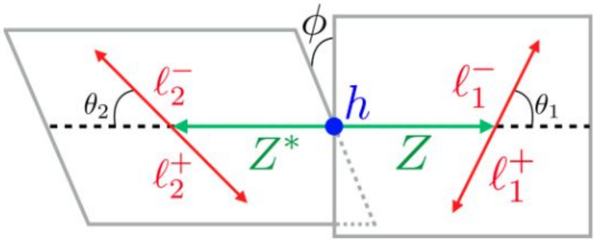

$$
\begin{aligned}
f_1 &= \sin^2(\theta_1)\sin^2(\theta_2)\\
f_2 &= (\cos^2(\theta_1)+1)(\cos^2(\theta_2)+1)\\
f_3 &= \sin(2\theta_1)\sin(2\theta_2)\cos(\phi)\\
f_4 &= (\cos^2(\theta_1)-1)(\cos^2(\theta_2)-1)\cos(2\phi)\\
f_5 &= \sin(\theta_1)\sin(\theta_2)\cos(\phi)\\
f_6 &= \cos(\theta_1)\cos(\theta_2)\\
f_7 &= (\cos^2(\theta_1)-1)(\cos^2(\theta_2)-1)\sin(2\phi)\\
f_8 &= \sin(\theta_1)\sin(\theta_2)\sin(\phi)\\
f_9 &= \sin(2\theta_1)\sin(2\theta_2)\sin(\phi),
\end{aligned}
$$

Mapping on to the Warsaw basis

$$\delta g_f^W = \frac{g}{\sqrt{2}} \frac{v^2}{\Lambda^2} c_{HF}^{(3)} + \frac{\delta m_Z^2}{m_Z^2} \frac{\sqrt{2} g c_{\theta_W}^2}{4 s_{\theta_W}^2}, \quad \text{where} \quad \frac{\delta m_Z^2}{m_Z^2} = \frac{v^2}{\Lambda^2}(2 t_{\theta_W} c_{WB} + \frac{c_{HD}}{2})$$

$$g_{Wf}^h = \sqrt{2} g \frac{v^2}{\Lambda^2} c_{HF}^{(3)}, \quad \delta \hat{g}_{WW}^h = \frac{v^2}{\Lambda^2} \left(c_{H\Box} - \frac{c_{HD}}{4} \right)$$

$$\kappa_{WW} = \frac{2v^2}{\Lambda^2} c_{HW}, \quad \tilde{\kappa}_{WW} = \frac{2v^2}{\Lambda^2} c_{H\tilde{W}}$$

$$\delta g_f^Z = -\frac{g' Y_f}{c_{\theta_W}} c_{WB} \frac{v^2}{\Lambda^2} - \frac{g}{c_{\theta_W}} \frac{v^2}{\Lambda^2} (|T_3^f| c_{HF}^{(1)} - T_3^f c_{HF}^{(3)} + (1/2 - |T_3^f|) c_{Hf}) c_{\theta_W}$$
$$+ \frac{\delta m_Z^2}{m_Z^2} \frac{g}{2 c_{\theta_W} s_{\theta_W}^2} (T_3 c_{\theta_W}^2 + Y_f s_{\theta_W}^2)$$

$$\delta \hat{g}_{ZZ}^h = \frac{v^2}{\Lambda^2} \left(c_{H\Box} + \frac{c_{HD}}{4} \right), \quad g_{Zf}^h = -\frac{2g}{c_{\theta_W}} \frac{v^2}{\Lambda^2} (|T_3^f| c_{HF}^{(1)} - T_3^f c_{HF}^{(3)} + (1/2 - |T_3^f|) c_{Hf})$$

$$\kappa_{ZZ} = \frac{2v^2}{\Lambda^2} (c_{\theta_W}^2 c_{HW} + s_{\theta_W}^2 c_{HB} + s_{\theta_W} c_{\theta_W} c_{HWB})$$

$$\tilde{\kappa}_{ZZ} = \frac{2v^2}{\Lambda^2} (c_{\theta_W}^2 c_{H\tilde{W}} + s_{\theta_W}^2 c_{H\tilde{B}} + s_{\theta_W} c_{\theta_W} c_{H\tilde{W}B})$$

$$\delta \hat{g}_{b\bar{b}}^h = -\frac{v^2}{\Lambda^2} \frac{v}{\sqrt{2} m_b} c_{y_b} + \frac{v^2}{\Lambda^2} (c_{H\Box} - \frac{c_{HD}}{4})$$

***VH*: Relations to the Warsaw Basis**

[Check out Rosetta: an operator basis translator for SMEFT]

EFT validity

- We estimate the scale of new physics for a measured g^h_{Zf}
- Example: Heavy $SU(2)_L$ triplet (singlet) vector W'^a (Z') couples to SM fermion current $\bar{f}\sigma^a\gamma_\mu f$ ($\bar{f}\gamma_\mu f$) with g_f and to the Higgs current $iH^\dagger\sigma^a \overleftrightarrow{D}_\mu H$ ($iH^\dagger \overleftrightarrow{D}_\mu H$) with g_H

$$g^h_{Zf} \sim \frac{g_H g g_f v^2}{\Lambda^2} \qquad g^h_{Zu_L,d_L} \sim \frac{g_H g^2 v^2}{2\Lambda^2}, \qquad g^h_{Zu_R,d_R} \sim \frac{g_H g g' Y_{u_R,d_R} v^2}{\Lambda^2}$$

- $\Lambda \rightarrow$ mass scale of vector and thus cut-off for low energy EFT
- Assumed g_f to be a combination of $g_B = g' Y_f$ and $g_W = g/2$ for universal case

Differential in energy: constraining the contact terms

Accidental cancellation of interference terms

LEP exclusion region

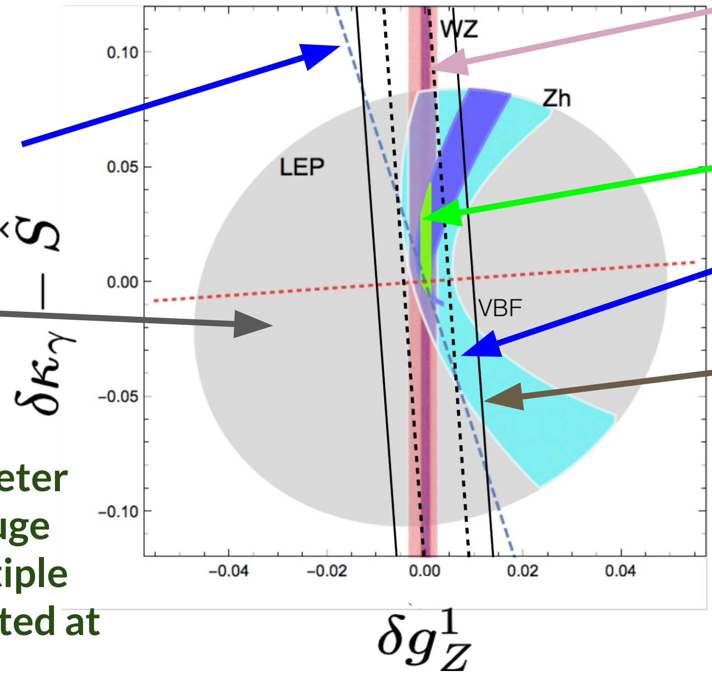

Exclusion from *WZ* [Franceschini et al, 2017]

Zh + *WZ* combined

Exclusion from *Zh* [SB, Englert, Gupta, Spannowsky, 2018]

WBF analysis in diphoton channel [Araz, SB, Gupta, Spannowsky, 2020]

A common parameter space in triple-gauge couplings for multiple channels - correlated at high energies

What about WW?

$\sigma_{Zh}^{SM}/\sigma_{Zbb}$ without cuts ~ 4.6/165

With regular cut-based analysis ~ 0.26

With BDT optimisation ~ 0.50

Higgs-Strahlung at the LHC (hZZ*/ hZff) (at high energies: contact interaction)

- We study the impact of constraining TGC couplings at higher energies
- We study the channel $pp \to Zh \to \ell^+\ell^- b\bar{b}$
- The backgrounds are SM $pp \to Zh$, $Zb\bar{b}$, $t\bar{t}$ and the fake $pp \to Zjj$ ($j \to b$ fake rate taken as 2%)
- Major background $Zb\bar{b}$ (b-tagging efficiency taken to be 70%)
- Boosted substructure analysis with fat-jets of $R = 1.2$ used

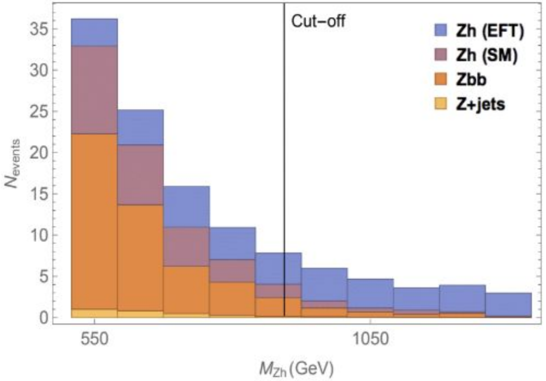

Cuts	Zbb	Zh (SM)
At least 1 fat jet with 2 B-mesons with $p_T > 15$ GeV	0.23	0.41
2 OSSF isolated leptons	0.41	0.50
80 GeV $< M_{\ell\ell} <$ 100 GeV, $p_{T,\ell\ell} > 160$ GeV, $\Delta R_{\ell\ell} > 0.2$	0.83	0.89
At least 1 fat jet with 2 B-meson tracks with $p_T > 110$ GeV	0.96	0.98
2 Mass drop subjets and ≥ 2 filtered subjets	0.88	0.92
2 b-tagged subjets	0.38	0.41
115 GeV $< m_h <$ 135 GeV	0.15	0.51
$\Delta R(b_i, \ell_j) > 0.4$, $\not{E}_T < 30$ GeV, $\lvert y_h \rvert < 2.5$, $p_{T,h/Z} > 200$ GeV	0.47	0.69

Event generator (hard-process simulation, resonance decay, PDF sampling, etc) → parton showering (ISR, FSR, etc) → hadronisation (baryon, meson production, etc) → underlying events (MPI) → detector simulation (smearing, efficiencies, energy deposition, etc) → event reconstruction (particle identification, jet clustering, MET, etc)

Differential in energy: constraining the contact terms

Single parameter fits from Zh

	Our 100 TeV Projection	Our 14 TeV projection	LEP Bound
$\delta g^Z_{u_L}$	± 0.0003 (± 0.0001)	± 0.002 (± 0.0007)	-0.0026 ± 0.0032
$\delta g^Z_{d_L}$	± 0.0003 (± 0.0001)	± 0.003 (± 0.001)	0.0023 ± 0.002
$\delta g^Z_{u_R}$	± 0.0005 (± 0.0002)	± 0.005 (± 0.001)	-0.0036 ± 0.0070
$\delta g^Z_{d_R}$	± 0.0015 (± 0.0006)	± 0.016 (± 0.005)	0.016 ± 0.0104
δg^Z_1	± 0.0005 (± 0.0002)	± 0.005 (± 0.001)	$-0.009^{+0.043}_{-0.042}$
$\delta \kappa_\gamma$	± 0.0035 (± 0.0015)	± 0.032 (± 0.009)	$-0.016^{+0.085}_{-0.096}$
$\hat{S}$	± 0.0035 (± 0.0015)	± 0.032 (± 0.009)	0.0004 ± 0.0007
W	± 0.0004 (± 0.0002)	± 0.003 (± 0.001)	-0.0003 ± 0.0006
Y	± 0.0035 (± 0.0015)	± 0.032 (± 0.009)	0.0000 ± 0.0006

Directions from *VBF*, *Zh*, *Wh*, and *WZ*

$$|(-0.04\ c^1_Q + 1.4\ c^{(3)}_Q + 0.1\ c_{uR} - 0.03\ c_{dR})\xi| < 0.003 \qquad [VBF]$$

$$|(-0.18\ c^1_Q + 1.3\ c^{(3)}_Q + 0.3\ c_{uR} - 0.1\ c_{dR})\xi| < 0.0005 \qquad [Zh]$$

$$|c^{(3)}_Q \xi| < 0.0004 \qquad [Wh]$$

$$-0.0004 < c^{(3)}_Q \xi < 0.0003 \qquad [WZ]$$

What about the W^+W^- direction?

Theory uncertainties in EFT analyses: operator truncation

Example showing the importance of truncation of operators to match specific models for a top-down approach!

[Dawson et al., 2022]

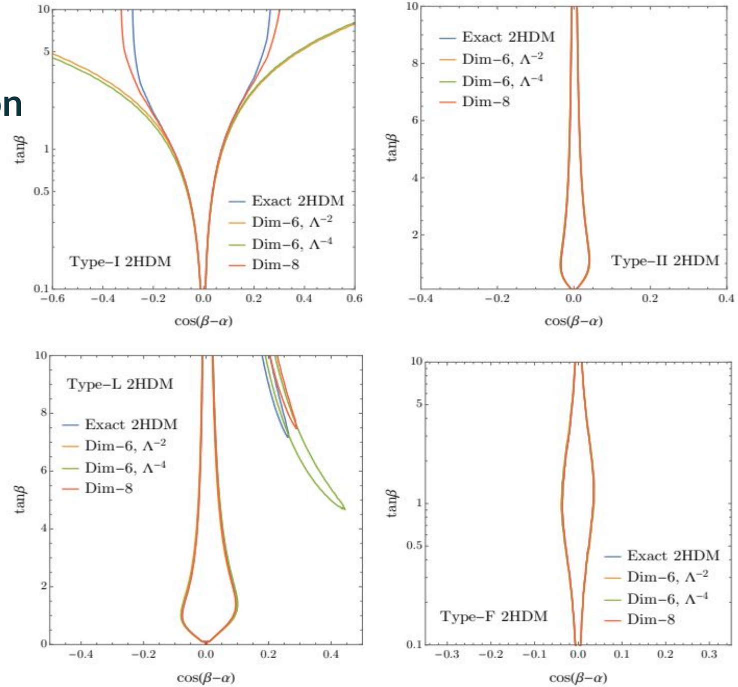

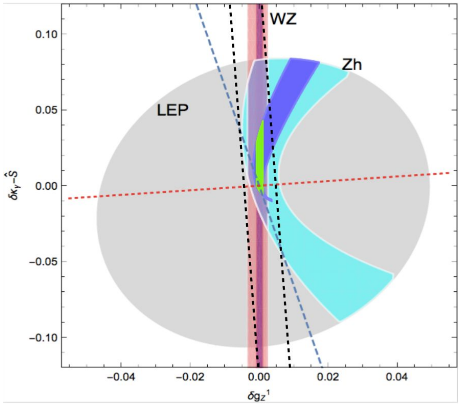

In parameter space of interest linear term dominates the squared term!

[SB, Englert, Gupta, Spannowsky, 2018]

Theory uncertainties in EFT analyses

1. **Ambiguities in operator coefficients → uncertainties in coefficients of remaining operators**

2. **Validity of perturbative expansion**

3. **Renormalisation Group Evolution (RGE) effects alter behaviour of theory under RGE → describes how EFT couplings vary with energy scales → uncertainties in predicted energy dependence of observables (If time permitting)**

4. **Can lead to inconsistencies while matching to a model**

Theory uncertainties in EFT analyses: TGCs

1. EFT operators contributing to anomalous charged triple gauge couplings (cTGCs) and anomalous neutral triple gauge couplings (nTGCs) $\longrightarrow$ **treated separately!**

2. For cTGCs, D8 operators are usually not considered.

3. For nTGCs, D8 operators are usually the first ones to show effects. Some such operators also contribute to cTGCs.

4. **Necessary to consider TGCs through a holistic approach!**

Theory uncertainties in EFT analyses: TGCs

1. **Relevant operators for TGCs at dimension-6 (D6)** $X^3 (X = W, B \text{ field strength tensor})$

2. **Relevant operators for TGCs at dimension-8 (D8)**

   $X^2\phi^2 D^2, X^2\psi^2 D \; (\phi = \text{Higgs field}, \psi = \text{fermion fields}, D = \text{covariant derivative})$

3. **These classes of operators contribute to TGCs and it is crucial to consider them in conjunction**

$$\dot{C}_G = (12c_{A,3} - 3b_{0,3})\, g_3^2 C_G \qquad \dot{C}_{\widetilde{G}} = (12c_{A,3} - 3b_{0,3})\, g_3^2 C_{\widetilde{G}}$$
$$\dot{C}_W = (12c_{A,2} - 3b_{0,2})\, g_2^2 C_W \qquad \dot{C}_{\widetilde{W}} = (12c_{A,2} - 3b_{0,2})\, g_2^2 C_{\widetilde{W}}$$

	$\phi^4 D^4$
$B^2\phi^2 D^2$	g_1^2
$W^2\phi^2 D^2$	g_2^2
$WB\phi^2 D^2$	$g_1 g_2$

	$\psi^2 B\phi^3$	$\psi^2 W\phi^3$	$\psi^2 G\phi^3$	$\psi^2\phi^2 D^3$
$B^2\phi^2 D^2$	0	0	0	g_1^2
$W^2\phi^2 D^2$	0	0	0	g_2^2
$WB\phi^2 D^2$	0	0	0	$g_1 g_2$

Alonso et al., 2013

Das Bakshi et al., 2022

Theory uncertainties in EFT analyses: RGE effects

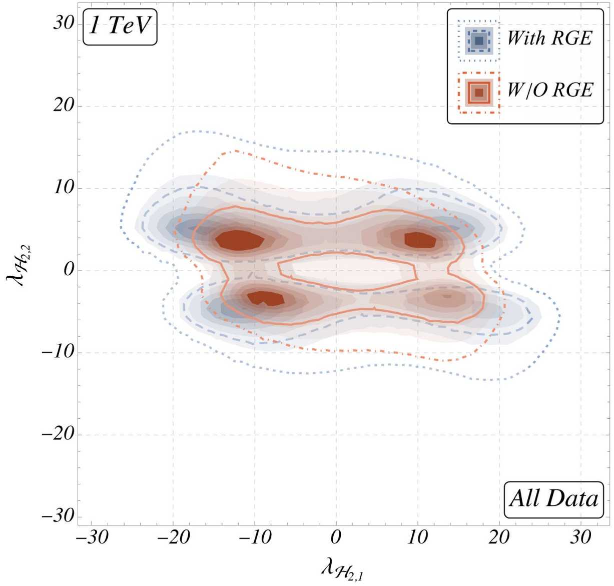

Usually, the running of the SMEFT operators are ignored which emerge at Λ. But, the measurements are at EW scale.

For 2HDM, 51 operators generated of which 14 are from RGE!

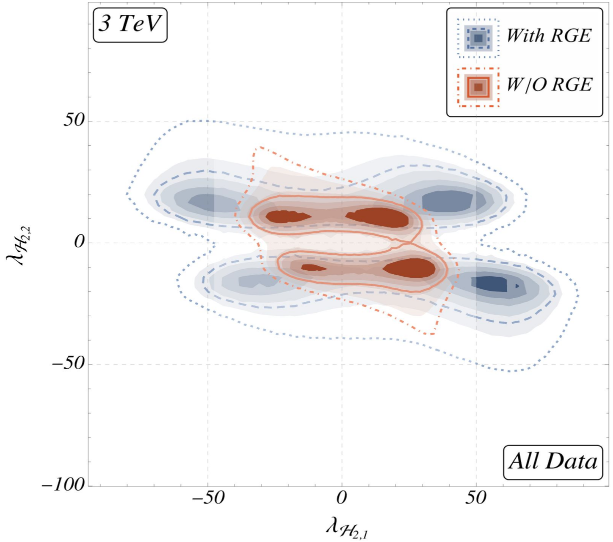

Increase in mass scale relaxes the parameter bounds!

[arXiv:2111.05876: Anisha, SB, et al, 2021]

Parameter space relaxed after considering RGE!

At LO

$$\mathcal{C}_i(M_Z) = \mathcal{C}_i(\Lambda) + \sum_j \frac{1}{16\pi^2}\gamma_{ij}\mathcal{C}_j(\Lambda)\log[\frac{M_Z}{\Lambda}]$$

$$\frac{d\mathcal{C}_i(\mu)}{d\log(\mu)} = \sum_j \frac{1}{16\pi^2}\gamma_{ij}\mathcal{C}_j$$

Leading log approximation

Theory uncertainties in EFT analyses: RGE effects

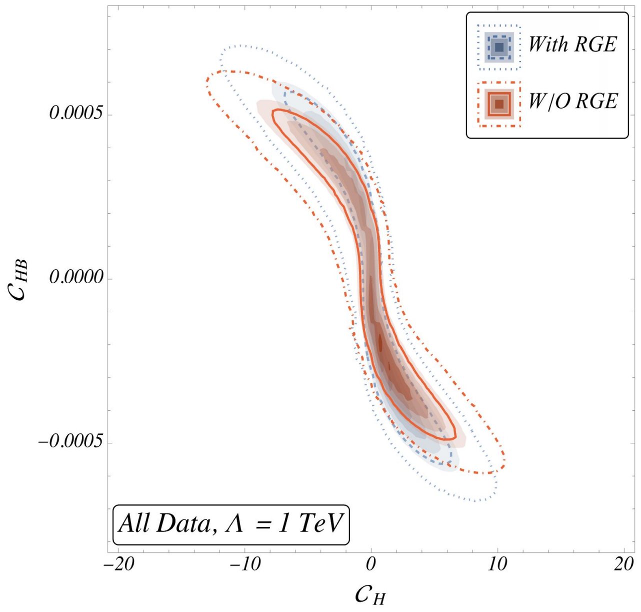

Usually, the running of the SMEFT operators ignored which emerge at Λ.
But, the measurements are at EW scale.

For 2HDM, 51 operators generated of which 14 are from RGE!

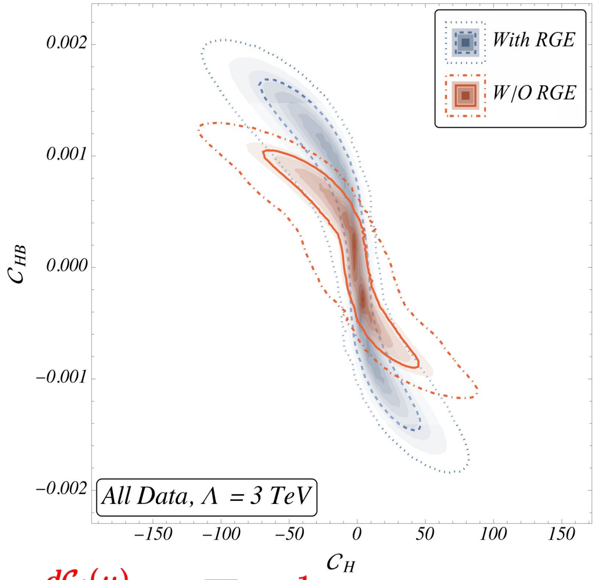

[arXiv:2111.05876: Anisha, SB, et al, 2021]

At LO

$$\mathcal{C}_i(M_Z) = \mathcal{C}_i(\Lambda) + \sum_j \frac{1}{16\pi^2}\gamma_{ij}\mathcal{C}_j(\Lambda)\log[\frac{M_Z}{\Lambda}]$$

$$\frac{d\mathcal{C}_i(\mu)}{d\log(\mu)} = \sum_j \frac{1}{16\pi^2}\gamma_{ij}\mathcal{C}_j$$

Theory uncertainties in EFT analyses: RGE effects

Usually, the running of the SMEFT operators ignored which emerge at Λ.
But, the measurements are at EW scale.

For 2HDM, 51 operators generated (top-down matching) of which 14 are from RGE! Examples (all suppressed by 16π²):

$\mathcal{O}_{uB}, \mathcal{O}_{uW}, \mathcal{O}_{dB}, \mathcal{O}_{dW}, \mathcal{O}_{eB}, \mathcal{O}_{eW}, \mathcal{O}_{Hud}$

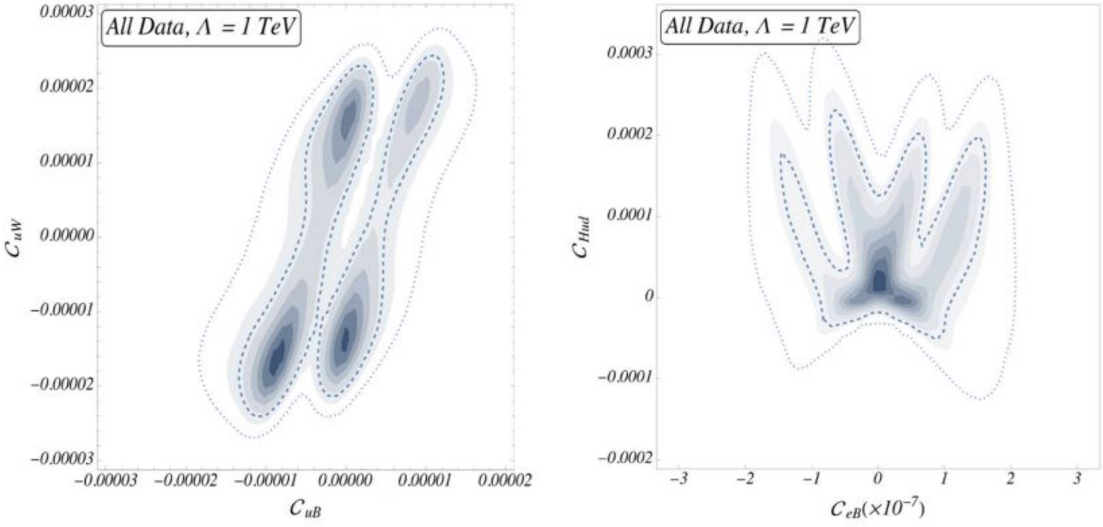

(a) $\mathcal{C}_{uB}$ - $\mathcal{C}_{uW}$ (b) $\mathcal{C}_{eB}$ - $\mathcal{C}_{Hud}$

[arXiv:2111.05876: Anisha, SB, et al, 2021]

Higgs Effective Field Theory (HEFT)

HEFT is the most general parametrisation of low-energy physics with only SM DOFs!!!

HEFT ⊃ SMEFT ⊃ SM **Is there any scenario where only HEFT can describe low-energy effects of BSM?**

1. Low-energy interactions only follow $U(1)_{em}$
2. The interactions can't tell us more about the properties of the microscopic theory
3. New non-decoupling strong dynamics → spontaneous EW symmetry breaking → Higgs-like scalar
4. SM not recovered when all BSM masses taken to infinity
5. Non-analyticity in Lagrangians can't be removed by field redefinitions → arises when **new states integrated out acquire mass from EWSB** → **violates decoupling** See Falkowski, Rattazzi

Unlike in the SMEFT, h is considered a gauge singlet and the Goldstone bosons, ω^a as an $SU(2)_L$ triplet. HEFT treats these separately → Goldstones embedded in Unitary matrix, U.

Part of the Lagrangian:

$$\mathcal{L}_{\text{HEFT}} \supset \frac{v^2}{4}\mathcal{F}(h)Tr\{D_\mu U^\dagger D^\mu U\}+\frac{1}{2}(\partial_\mu h)^2 - V(h) - \frac{v}{\sqrt{2}}(\bar{u}^i_L \bar{d}^i_L)\mathcal{F}(h)\begin{pmatrix} y^u_{ij}u^j_R \\ y^d_{ij}d^j_R \end{pmatrix} + \text{h.c.}$$

$$\mathcal{F}(h) = 1 + 2a\frac{h}{v} + b\frac{h^2}{v^2} + \ldots$$

$$V(h) = \frac{1}{2}m_h^2 v^2(1 + d_3\frac{h}{v} + \frac{d_4}{4}\frac{h^2}{v^2}) + \ldots$$

$$D_\mu U = \partial_\mu U + igW^a_\mu \frac{\sigma^a}{2}U - ig'U\frac{\sigma^3}{2}B_\mu$$

See geometric interpretation of HEFT with Higgs and Goldstone bosons as coordinates of Riemannian manifold

Motivated by Cohen et al.

SMEFT versus HEFT

SMEFT

1. **Most general set of local operators invariant under $SU(3)_C X\ SU(2)_L X\ U(1)_Y$**

2. **Operators suppressed by powers of new-physics scale, Λ**

3. **Low energy states modelled using fields transforming linearly under aforementioned symmetries**

4. **Observed Higgs, *h*, is a component of an electroweak doublet scalar, *H***

5. **More restrictive symmetry structure → less number of parameters which are correlated**

HEFT

1. **Manifest gauge symmetry is $SU(3)_C X\ U(1)_{em}$**

2. **Operators suppressed by electroweak breaking scale, *v***

3. **The $SU(2)_L X\ U(1)_Y$ symmetry is non-linearly realised using a multiplet of Goldstone bosons**

4. **No relation between *h* and the Goldstone bosons**

5. **Less restrictive symmetry structure → more number of uncorrelated parameters**

CP symmetry

1. CP refers to the “Charge Parity” symmetry which involves two fundamental symmetries
2. Charge Conjugation (C): Operation involves changing particles to antiparticles and vice versa
3. Parity Transformation (P): Operation involves inversion of spatial coordinates
4. CP symmetry: Operation C followed by P; reflects the transformation of a particle process into its antiparticle process with spatial coordinates inverted
5. A particle physics process is CP symmetric if the laws of physics governing that process remain unchanged when particles are replaced by their antiparticles and spatial coordinates are inverted
6. CP violation is important in particle physics; in certain processes involving the weak force, CP is not conserved; first observed in the neutral kaon decays in the 1960s (Nobel Prize in Physics, 1980)
7. Crucial aspect of understanding the matter-antimatter asymmetry observed in the universe; study of CP violation helps physicists explore the origins of this asymmetry.

CP violation

1. Explaining observed baryon asymmetry requires sufficient charge (C) and parity (P) violation → one of the three necessary Sakharov conditions

2. In SM, only source of CP-violation is a complex phase in the CKM matrix (quark mixing) → not enough to explain baryon asymmetry

3. CP-violation may exist in the neutrino and strong sectors

4. Can there be (enough) CP-violation in the Higgs sector?

CP violation in the Higgs-Gauge sector (*VBF h, h$\longrightarrow$ ZZ**$\longrightarrow$ 4l*)

Operator	Structure	Coupling
	Warsaw Basis	
$O_{\Phi\tilde{W}}$	$\Phi^\dagger\Phi\tilde{W}^I_{\mu\nu}W^{\mu\nu I}$	$c_{H\widetilde{W}}$
$O_{\Phi\tilde{W}B}$	$\Phi^\dagger\tau^I\Phi\tilde{W}^I_{\mu\nu}B^{\mu\nu}$	$c_{H\widetilde{W}B}$
$O_{\Phi\tilde{B}}$	$\Phi^\dagger\Phi\tilde{B}_{\mu\nu}B^{\mu\nu}$	$c_{H\tilde{B}}$
	Higgs Basis	
$O_{hZ\tilde{Z}}$	$hZ_{\mu\nu}\tilde{Z}^{\mu\nu}$	$\tilde{c}_{zz}$
$O_{hZ\tilde{A}}$	$hZ_{\mu\nu}\tilde{A}^{\mu\nu}$	$\tilde{c}_{z\gamma}$
$O_{hA\tilde{A}}$	$hA_{\mu\nu}\tilde{A}^{\mu\nu}$	$\tilde{c}_{\gamma\gamma}$

CP-odd dimension-6 operators contributing to h $\rightarrow$ 4l final state

EFT framework! More details in the EFT sessions.

1. ATLAS assumes a common parametrization for CP-violation searches, denoted by $\tilde{d}$

2. It was considered that different contributions from various electroweak gauge boson fusion processes could not be distinguished experimentally

3. They assumed

$$c_{H\tilde{W}} = c_{H\tilde{B}} = \frac{\Lambda^2}{v^2}\tilde{d}, c_{H\tilde{W}B} = 0$$

$$\tilde{c}_{z\gamma} = 0, \tilde{c}_{\gamma\gamma} = \sin^2\theta_W \cos^2\theta_W \tilde{c}_{zz}$$

CP violation in the Higgs-Gauge sector (*VBF h, h$\longrightarrow$ ZZ*$\longrightarrow$ 4l*)

1. To test CP-violation, ATLAS considered the Optimal Observables (defined below) against the various CP-odd operators

2. Cross-section proportional to $|\mathcal{M}|^2 = |\mathcal{M}_{SM}|^2 + 2\sum_i \frac{c_i}{\Lambda^2}\mathcal{R}(\mathcal{M}^*_{SM}\mathcal{M}_{BSM,i}) + \sum_i\sum_j \frac{c_i c_j}{\Lambda^4}\mathcal{R}(\mathcal{M}^*_{BSM,i}\mathcal{M}_{BSM,j})$

3. The first and the last terms are CP-even. The second term is the interference term and it is CP-odd and hence a suitable probe for studying CP-violation

4. Optimal Observable defined as $\mathcal{OO} = \frac{2\mathcal{R}(\mathcal{M}^*_{SM}\mathcal{M}_{BSM})}{|\mathcal{M}_{SM}|^2}$ and has a symmetric distribution

   with 0 mean in the absence of CP-violation. Any asymmetry would be direct evidence of CP-violation
5. Production and decay level Optimal Observables are computed. For the production level ones, PDF weighting done over various partonic modes and summed. For the decay level, matrix element for the Higgs boson decay reconstructed from four-momenta of the four leptons

CP violation in the Higgs-Gauge sector (*VBF h, h→ ZZ* → 4l*)

EFT coupling parameter	Expected 68% CL	Expected 95% CL	Observed 68% CL	Observed 95% CL	Best-fit value	SM p-value	Fit typ
$c_{H\tilde{B}}$	[−0.18, 0.19]	[−0.37, 0.37]	[−0.42, 0.31]	[−0.61, 0.54]	−0.078	0.86	decay
$c_{H\tilde{W}B}$	[−0.36, 0.36]	[−0.72, 0.72]	[−0.56, 0.53]	[−0.97, 0.98]	−0.017	[illegible]	decay
$c_{H\tilde{W}}$	[−0.63, 0.63]	[−1.26, 1.28]	[−0.07, 1.09]	[−0.81, 1.54]	0.60	0.37	comb
$\tilde{d}$	[−0.009, 0.009]	[−0.018, 0.018]	[−0.017, 0.014]	[−0.026, 0.025]	−0.003	0.86	decay
$\tilde{c}_{zz}$	[−0.77, 0.79]	[−2.4, 2.4]	[0.37, 1.21]	[−1.20, 1.75]	0.78	0.11	prod
$\tilde{c}_{z\gamma}$	[−0.47, 0.47]	[−0.76, 0.76]	[−0.54, 0.54]	[−0.84, 0.83]	0.083	0.93	decay
$\tilde{c}_{\gamma\gamma}$	[−0.38, 0.38]	[−0.76, 0.77]	[−0.52, 0.48]	[−0.99, 0.93]	−0.01	0.99	decay

Sensitive to both production and decay! One operator at a time

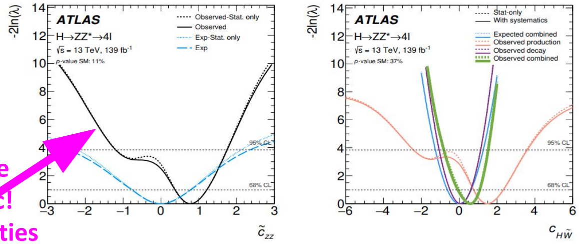

(a) $\tilde{c}_{zz}$ production
(b) $c_{H\tilde{W}}$

Small excess of VBF candidates at positive $\tilde{c}_{zz}$. Non-parabolic! Systematic uncertainties large (ggF PS)

***p*-value for agreement with SM is 0.11 (0.37) for the $\tilde{c}_{zz}$ ($c_{H\tilde{W}}$) coupling NLL scan (Λ = 1 TeV)**

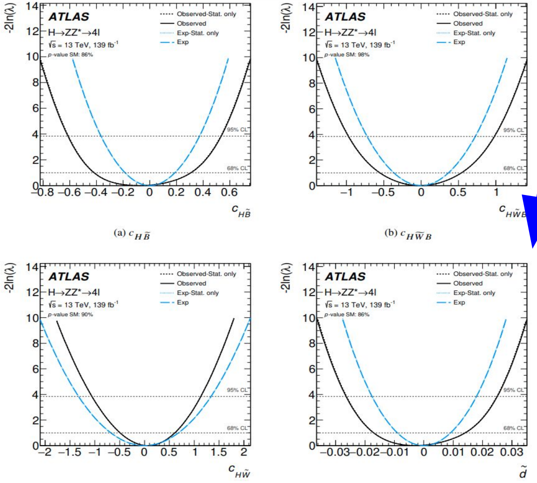

(a) $c_{H\tilde{B}}$
(b) $c_{H\tilde{W}B}$
(c) $c_{H\tilde{W}}$
(d) $\tilde{d}$

Decay only fits; one operator at a time

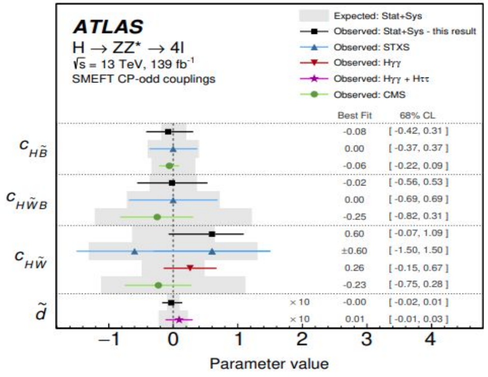

2D contours!

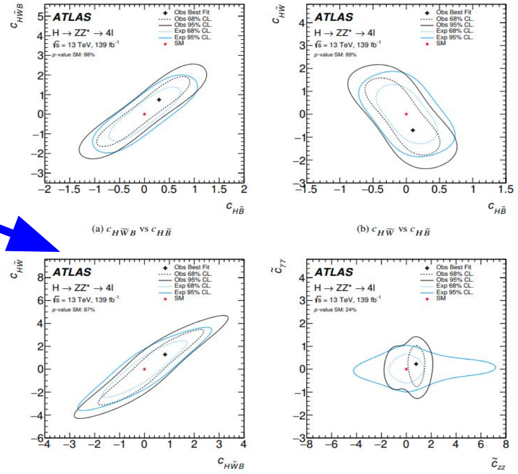

(a) $c_{H\tilde{W}B}$ vs $c_{H\tilde{B}}$
(b) $c_{H\tilde{W}}$ vs $c_{H\tilde{B}}$
(c) $c_{H\tilde{W}}$ vs $c_{H\tilde{W}B}$
(d) $\tilde{c}_{\gamma\gamma}$ vs $\tilde{c}_{zz}$

Catani-Seymour

The Catani-Seymour subtraction method, including the use of the insertion operator \(\mathbf{I}(\epsilon) \), was originally developed for handling infrared (IR) divergences in Quantum Chromodynamics (QCD) calculations. However, the principles behind the subtraction method can be extended and applied to other gauge theories, including electroweak (EW) theory, for next-to-leading-order (NLO) calculations.

Application to Electroweak Calculations

When dealing with NLO corrections in electroweak (EW) theory, similar challenges arise due to IR divergences from soft and collinear photons (and sometimes Z bosons in specific processes). The Catani-Seymour subtraction method can be adapted to manage these divergences as follows:

1. Photon Emission: Just as gluons can be soft or collinear in QCD, photons can be emitted in a soft or collinear manner, leading to IR divergences. The subtraction terms in the Catani-Seymour method can be modified to account for the specific kinematics and coupling structures of photon emissions.

Catani Seymour

2. Universal Structures: The structure of IR divergences has universal properties that apply across different gauge theories. The key idea of constructing counterterms that locally approximate the behavior of the matrix elements in singular regions remains valid.

3. Insertion Operators: In the EW context, the insertion operator $\mathbf{I}(\epsilon)$ must be redefined to include the contributions from the EW interactions. This involves recalculating the kinematic factors $\mathcal{V}_{ij}(\epsilon)$ to reflect the dynamics of photons (and possibly other weak bosons).

4. Mixed QCD-EW Corrections: In processes involving both QCD and EW corrections, a combined subtraction scheme can be employed. This involves constructing subtraction terms that handle both QCD and EW singularities simultaneously, ensuring a consistent treatment of all IR divergences.

Catani Seymour Insertion Operator

$$\boldsymbol{I}(\epsilon, \mu^2; \kappa, \{\alpha_{\text{dip}}\}) = -\frac{\alpha}{2\pi}\frac{(4\pi)^\epsilon}{\Gamma(1-\epsilon)}\sum_i\sum_{k\neq i}\boldsymbol{I}_{ik}(\epsilon, \mu^2; \kappa, \{\alpha_{\text{dip}}\})$$

Contains all flavour-diagonal endpoint contributions and cancels all divergences present in the one-loop matrix elements.

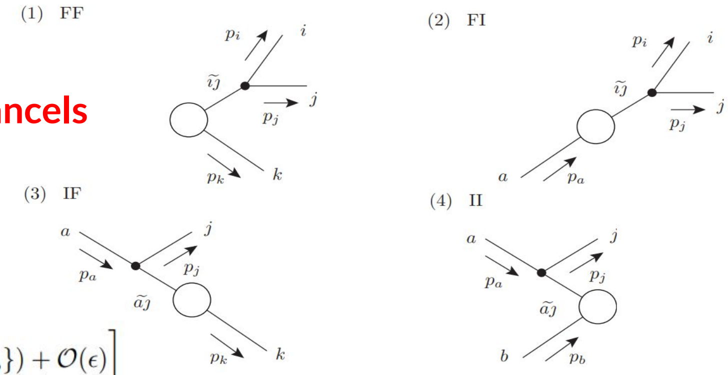

Regularisation scale

Charge insertion operator

$$\boldsymbol{I}_{ik}(\epsilon, \mu^2; \kappa, \{\alpha_{\text{dip}}\}) = \boldsymbol{Q}^2_{ik}\left[\mathcal{V}_{ik}(\epsilon, \mu^2; \kappa) + \Gamma_i(\epsilon, \mu^2) + \gamma_i\left(1 + \ln\frac{\mu^2}{s_{ik}}\right) + K_i + A^I_{ik}(\{\alpha_{\text{dip}}\}) + \mathcal{O}(\epsilon)\right]$$

***i*, *k* label the emitter and spectator, respectively**

Divergences

Schoenherr, 2018

$$\mathcal{V}_{ik}(\epsilon, \mu^2; \kappa) = \begin{cases} Q_i^2\left(\frac{\mu^2}{s_{ik}}\right)^\epsilon\left[\mathcal{V}^{(\text{S})}_{ik}(\epsilon) + \mathcal{V}^{(\text{NS})}_{ik}(\kappa) - \frac{\pi^2}{3}\right] & i \neq \gamma \\ \mathcal{V}^{(\text{NS})}_{\gamma k}(\kappa) & i = \gamma \end{cases}$$

Angular observables: Zh and Wh production at the LHC (example)

$$\sum_{L,R} |\mathcal{A}(\hat{s},\Theta,\theta,\varphi)|^2 = a_{LL}\sin^2\Theta\sin^2\theta + a^1_{TT}\cos\Theta\cos\theta$$
$$+ a^2_{TT}(1+\cos^2\Theta)(1+\cos^2\theta) + \cos\varphi\sin\Theta\sin\theta$$
$$\times (a^1_{LT} + a^2_{LT}\cos\theta\cos\Theta) + \sin\varphi\sin\Theta\sin\theta$$
$$\times (\tilde{a}^1_{LT} + \tilde{a}^2_{LT}\cos\theta\cos\Theta) + a_{TT'}\cos 2\varphi\sin^2\Theta\sin^2\theta$$
$$+ \tilde{a}_{TT'}\sin 2\varphi\sin^2\Theta\sin^2\theta$$

Q: Are the LO theoretical shapes preserved upon the inclusion of NLO effects, radiations, showering, experimental cuts, etc.?

A: For the azimuthal angles, they are.

Angular moments a^2_{LT} and $\tilde{a}^2_{LT}$ after weighting each event by the sign of $\sin 2\Theta \sin 2\theta$

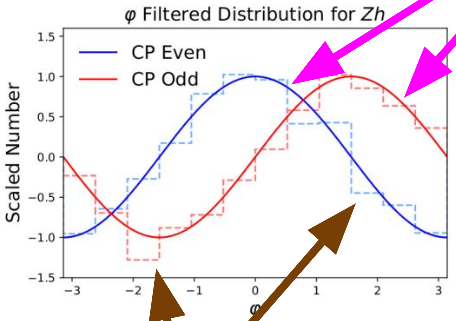

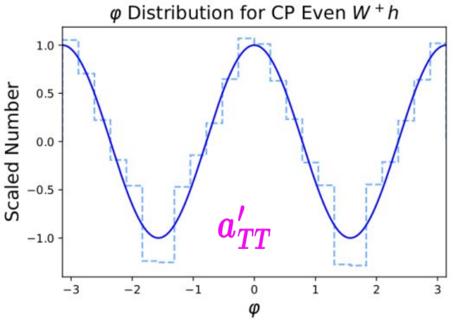

- Ambiguity in neutrino p_z

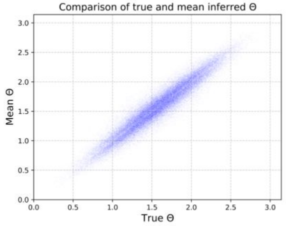

Assuming on-shell W!

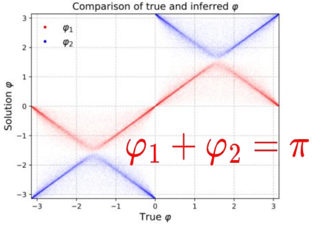

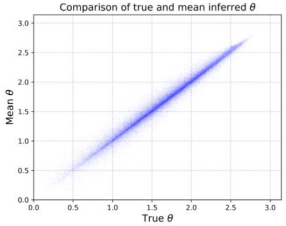

SB, Gupta, Reiness, Seth, Spannowsky, 2020

Monte Carlo samples: showering, hadronisation, passing all selection cuts

Method of Moments

- An analog of Fourier analysis utilised to extract angular moments
- Our squared amplitude can be parametrised as,
  $|\mathcal{A}|^2 = \sum_i a_i(E) f_i(\Theta, \theta, \varphi)$
- We look for weight functions, $w_i(\Theta, \theta, \varphi)$, such that
  $< w_i | f_i >= \int d(\Theta, \theta, \varphi) w_i f_j = \delta_{ij}$
- One can then pick out the angular moments, a_i as
  $a_i = \int d(\Theta, \theta, \varphi) |\mathcal{A}|^2 w_i$

Method of Moments

- For the set of basis functions, we get the following matrix

$$M = \begin{pmatrix} \frac{512\pi}{225} & 0 & \frac{128\pi}{25} & 0 & 0 & 0 & 0 & 0 & 0 \\ 0 & \frac{8\pi}{9} & 0 & 0 & 0 & 0 & 0 & 0 & 0 \\ \frac{128\pi}{25} & 0 & \frac{6272\pi}{225} & 0 & 0 & 0 & 0 & 0 & 0 \\ 0 & 0 & 0 & \frac{16\pi}{9} & 0 & 0 & 0 & 0 & 0 \\ 0 & 0 & 0 & 0 & \frac{16\pi}{225} & 0 & 0 & 0 & 0 \\ 0 & 0 & 0 & 0 & 0 & \frac{16\pi}{9} & 0 & 0 & 0 \\ 0 & 0 & 0 & 0 & 0 & 0 & \frac{16\pi}{225} & 0 & 0 \\ 0 & 0 & 0 & 0 & 0 & 0 & 0 & \frac{256\pi}{225} & 0 \\ 0 & 0 & 0 & 0 & 0 & 0 & 0 & 0 & \frac{256\pi}{225} \end{pmatrix}$$

- $w_i \propto f_i$ except for $i = 1, 3$
- We rotate the (1,3) system to an orthogonal basis
- Using discrete method, we find: $a_i(M) = \frac{\hat{N}}{N} \sum_{n=1}^{N} w_i(\Theta_n, \theta_n, \varphi_n)$
- Events divided in bins of final state invariant mass ($M \rightarrow$ central value of bin), $N(M)(N(\hat{M})) \rightarrow$ number of MC (actual) events in that bin for a fixed integrated luminosity

Angular observables: Vh $\longrightarrow$ 2lbb and ggF (h $\longrightarrow$ ZZ* $\longrightarrow$ 4l)

$Vh\ \left(\frac{d\sigma}{dEd\Theta d\theta d\varphi}\right)$

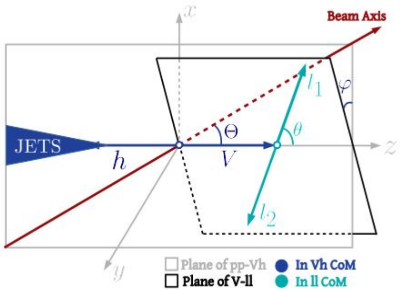

$$f_{LL} = S_\Theta^2 S_\theta^2,$$
$$f_{TT}^1 = C_\Theta C_\theta,$$
$$f_{TT}^2 = (1 + C_\Theta^2)(1 + C_\theta^2),$$
$$f_{LT}^1 = C_\varphi S_\Theta S_\theta,$$
$$f_{LT}^2 = C_\varphi S_\Theta S_\theta C_\Theta C_\theta,$$
$$\tilde{f}_{LT}^1 = S_\varphi S_\Theta S_\theta,$$
$$\tilde{f}_{LT}^2 = S_\varphi S_\Theta S_\theta C_\Theta C_\theta,$$
$$f_{TT'} = C_{2\varphi} S_\Theta^2 S_\theta^2,$$
$$\tilde{f}_{TT'} = S_{2\varphi} S_\Theta^2 S_\theta^2\,,$$

$ggF\ \left(\frac{d\sigma}{dEd\theta_1 d\theta_2 d\phi}\right)$

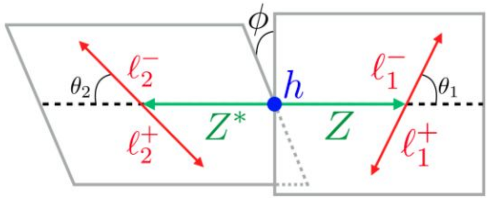

$$f_1 = \sin^2(\theta_1)\sin^2(\theta_2)$$
$$f_2 = (\cos^2(\theta_1) + 1)(\cos^2(\theta_2) + 1)$$
$$f_3 = \sin(2\theta_1)\sin(2\theta_2)\cos(\phi)$$
$$f_4 = (\cos^2(\theta_1) - 1)(\cos^2(\theta_2) - 1)\cos(2\phi)$$
$$f_5 = \sin(\theta_1)\sin(\theta_2)\cos(\phi)$$
$$f_6 = \cos(\theta_1)\cos(\theta_2)$$
$$f_7 = (\cos^2(\theta_1) - 1)(\cos^2(\theta_2) - 1)\sin(2\phi)$$
$$f_8 = \sin(\theta_1)\sin(\theta_2)\sin(\phi)$$
$$f_9 = \sin(2\theta_1)\sin(2\theta_2)\sin(\phi),$$

SB, Englert, Gupta, Spannowsky, 2018

SB, Gupta, Ochoa-Valeriano, Spannowsky, Venturini, 2020

Angular observables: Gluon fusion in golden channel (example)

- Angular differential distributions, modified in the EFT

$$a_1 = \mathcal{G}^4\left((1+\delta a) + \frac{b m_{Z^*}\gamma_b^2}{m_Z\gamma_a}\right)^2$$
$$a_2 = \mathcal{G}^4\left(\frac{(1+\delta a)^2}{2\gamma_a^2} + \frac{2c^2 m_{Z^*}^2\gamma_b^2}{m_Z^2\gamma_a^2}\right)$$
$$a_3 = -\mathcal{G}^4\left(\frac{1+\delta a}{2\gamma_a} + \frac{b m_{Z^*}\gamma_b^2}{2m_Z\gamma_a}\right)^2$$
$$a_4 = \mathcal{G}^4\left(\frac{(1+\delta a)^2}{2\gamma_a^2} - \frac{2c^2 m_{Z^*}^2\gamma_b^2}{m_Z^2\gamma_a^2}\right)$$
$$a_5 = -\epsilon^2\mathcal{G}^4\left(\frac{2(1+\delta a)^2}{\gamma_a} + \frac{2(1+\delta a) b m_{Z^*}\gamma_b^2}{m_Z\gamma_a^2}\right)$$
$$a_6 = \epsilon^2\mathcal{G}^4\left(\frac{2(1+\delta a)^2}{\gamma_a^2} + \frac{8c^2 m_{Z^*}^2\gamma_b^2}{m_Z^2\gamma_a^2}\right)$$
$$a_7 = \mathcal{G}^4\frac{2(1+\delta a) c m_{Z^*}\gamma_b}{m_Z\gamma_a^2}$$
$$a_8 = -\epsilon^2\mathcal{G}^4\left(\frac{4(1+\delta a) c m_{Z^*}\gamma_b}{m_Z\gamma_a} + \frac{4bc m_{Z^*}^2\gamma_b^3}{m_Z^2\gamma_a^2}\right)$$
$$a_9 = \mathcal{G}^4\left(\frac{(1+\delta a) c m_{Z^*}\gamma_b}{m_Z\gamma_a} + \frac{bc m_{Z^*}^2\gamma_b^3}{m_Z^2\gamma_a^2}\right),$$

1 → SM

$$\delta a = \delta\hat{g}^h_{ZZ} - \kappa_{ZZ}\gamma_a\frac{m_{Z^*}}{m_Z}\frac{m_Z^2 - m_{Z^*}^2}{2m_Z^2}$$
$$b = \kappa_{ZZ}$$
$$c = -\frac{\tilde{\kappa}_{ZZ}}{2}$$

$$\mathcal{G}^4 = ((g^Z_{l_L})^2 + (g^Z_{l_R})^2)((g^{Z^*}_{l_L})^2 + (g^{Z^*}_{l_R})^2)$$
$$\epsilon^2\mathcal{G}^4 = ((g^Z_{l_L})^2 - (g^Z_{l_R})^2)((g^{Z^*}_{l_L})^2 - (g^{Z^*}_{l_R})^2),$$
↓

Small → a_5, a_6 **and** a_8 **suppressed**

a_7, a_8, a_9 **CP-odd**

SB, Gupta, Ochoa-Valeriano, Spannowsky, Venturini, 2020

[Slide courtesy Elena Venturini]